FERRITES, MAGNETIC, H. F.

Report No. 54 Contract No. 6

Signal Corps Contract DA-36-039
SC-89222

Dept. of Army Project 3A99-15-006-02

Third Quarterly Report

1 December 1962 to 28 February 1963

U. S. ARMY ELECTRONICS RESEARCH AND DEVELOPMENT LABORATORY
FORT MONMOUTH, NEW JERSEY

DIVISION OF INDIANA GENERAL CORPORATION

INDIANA GENERAL CORPORATION
ELECTRONICS DIVISION
RESEARCH DEPARTMENT
KEASBEY, NEW JERSEY — Telephone VAlley 6-5100,

FERRITES, MAGNETIC, H.F.

Report No. 54 Contract No. 6
Signal Corps Contract DA-36-039
SC-89222

Dept. of Army Project 3A99-15-006-02

THIRD QUARTERLY REPORT

1 December 1962 to 28 February 1963

OBJECT: Conduct investigations and develop magnetic high frequency core materials.

REPORTED BY: Dr. Eberhard Schwabe, Physicist - Supervisor
Dr. Kurt F. Wetzel, Chemist
Daniel Sullivan, Ceramic Engineer
William Stollar, Ceramic Engineer
Charles O'Neill, Chemist

TABLE OF CONTENTS

Title Page . . . . . .Page 1

Table of Contents . . . . . Page 2

List of Graphs . . . . . .Page 3

List of Tables . . . . . .Page 5

Abstracts . . . . . Page 6

Foreword . . . . . .Page 8

PART I. MANGANESE-ZINC FERRITES

SECTION A

High Purity Materials in Relation to Temperature Stability and $\mu_o Q$ Product . . . . . Page 15

Disaccommodation (Aging) of Mn-Zn Ferrites . . . . . Page 18

SECTION B

Investigation of the Effects of Particle and Grain Size on $\mu_o Q$, Temperature Coefficient and Disaccommodation of Mn-Zn Ferrites. . . . . Page 20

PART II. NICKEL-ZINC FERRITES

SECTION A . . . . . Page 22

SECTION B

Investigation of the Effects of Particle and Grain Size on $\mu_o Q$, Temperature Coefficient and Disaccommodation of Ni-Zn Ferrites . . . . . Page 22

PART III Research Planned for Next Quarter . . . . . Page 24

PART IV Manhours Spent on Contract for the Period: 1 December 1962 to 28 February 1963 . . . . . Page 25

LIST OF GRAPHS

GRAPHS	DESCRIPTION
539	% $\Delta\mu_o/\mu_o$ vs. Temperature for MF-8649-1 (Preparation A, B, C, D). Batch Type Kiln Harrop #103, Firing No. 1. Peak Temperature 2480°F, Cooling in N_2.
594	% $\Delta\mu_o/\mu_o$ vs. Temperature for MF-8649-2 (Preparation A, B, C, D). Batch Type Kiln Harrop #103, Firing No. 1. Peak Temperature 2480°F, Cooling in N_2.
595	% $\Delta\mu_o/\mu_o$ vs. Temperature for MF-8649-3 (Preparation A, B, C, D). Batch Type Kiln Harrop #103, Firing No. 1. Peak Temperature 2480°F, Cooling in N_2.
596	% $\Delta\mu_o/\mu_o$ vs. Temperature for MF-8649-1 (Preparation A, B, C, D). Batch Type Kiln Harrop #101, Firing 58F (No. 2), Peak Temperature 2400°F, Cooling in N_2.
597	% $\Delta\mu_o/\mu_o$ vs. Temperature for MF-8649-2 (Preparation A, B, C, D). Batch Type Kiln Harrop #101, Firing 58 F (No. 2), Peak Temperature 2400°F, Cooling in N_2.
598	% $\Delta\mu_o/\mu_o$ vs. Temperature for MF-8649-3 (Preparation A, B, C, D). Batch Type Kiln Harrop #101, Firing 58F (No. 2), Peak Temperature 2400°F, Cooling in N_2.
599	% $\Delta\mu_o/\mu_o$ vs. Temperature for MF-9649-1 (Preparation A, B, C, D). Batch Type Kiln Harrop #101, Firing 64F (No. 6), Peak Temperature 2380°F, Cooling in N_2.
600	% $\Delta\mu_o/\mu_o$ vs. Temperature MF-8649-2 (Preparation A, B, C, D). Batch Type Kiln Harrop #101, Firing 64F (No. 6), Peak Temperature 2380°F, Cooling in N_2.
601	% $\Delta\mu_o/\mu_o$ vs. Temperature MF-8649-3 (Preparation A, B, C, D). Batch Type Kiln Harrop #101, Firing 64F (No. 6), Peak Temperature 2380°F, Cooling in N_2.
602	Disaccommodation - MF-8401-1, 2, 3, $-\Delta\mu_o/\mu_o$(%) vs. Time (sec) at Varying Temperatures
603	Disaccommodation - MF-8402-1, 2, 3, $-\Delta\mu_o/\mu_o$ (%) vs. Time (sec) at Varying Temperatures.

LIST OF GRAPHS (Continued)

GRAPHS	DESCRIPTION
604	Disaccommodation - MF-8400-1, 2, 3, $-\Delta\mu_o/\mu_o$ (%) vs. Time (sec) at Varying Temperatures
605	Disaccommodation $-\Delta\mu_o/\mu_o$ (%) vs. Time (sec) at $\sim$ 25°C
606	Disaccommodation - MF-4373-A, $-\Delta\mu_o/\mu_o$ (%) vs. Time (sec) at Varying Temperatures
607	Disaccommodation - MF-4373-A, $-\Delta\mu_o/\mu_o$ (%) vs. Time (sec) at $\sim$ 25°C
608	Coercive Force vs. Milling Time for Material MF-8644-1, 8644-4
609	H_c vs. Powder Particle Size for Material MF-8644-1, 8644-4
610	$\mu_o Q$ vs. Frequency for Material MF-8644-1, 8644-4, Milling Time 2 hours
611	$\mu_o Q$ vs. Frequency for Material MF-8644-1, 8644-4, Milling Time 4 hours
612	$\mu_o Q$ vs. Frequency for Material MF-8644-1, 8644-4, Milling Time 8 hours
613	$\mu_o Q$ vs. Frequency for Material MF-8644-1, 8644-4, Milling Time 16 hours
614	$\mu_o Q$ vs. Frequency for Material MF-8644-1, 8644-4, Milling Time 32 hours
615	$\mu_o Q$ vs. Frequency for Material MF-8644-1, 8644-4, Milling Time 64 hours
616	Coercive Force vs. Milling Time Ni-Zn Ferrites 9000-9001, Calcined at 2400°F.
617	Particle Size vs. Milling Time Ni-Zn Ferrites 9000-9001, Calcined at 2400°F
618	Coercive Force vs. Milling Time Ni-Zn Ferrites 9000-9001, Calcined at 2200°F.

FIGURE	DESCRIPTION
1	Circuit Diagram - Intrinsic Coercive Force Measurement
2	Circuit Design - Disaccommodation Measurement

LIST OF TABLES

TABLES	DESCRIPTION
275	Test Series - MF-8649 - a) Schedule of different types of preparation and its effect upon the iron oxide ratio. b) Schedule of firings.
276	Magnetic properties of MF-8649-1 obtained from four different types of preparation and from five different firings. Measurements of μ_o and Q at frequencies of from 100 to 300 kc/s.
277	Magnetic properties of MF-8649-2 obtained from four different types of preparation and from five different firings. Measurements of μ_o and Q at frequencies of from 100 to 300 kc/s.
278	Magnetic properties of MF-8649-3 obtained from four different types of preparation and from five different firings. Measurements of μ_o and Q at frequencies of from 100 to 300 kc/s.

ABSTRACTS

PART I MANGANESE-ZINC FERRITES

SECTION A

High Purity Mn-Zn Ferrites

The investigation described in Part I of Report No. 53 was continued. Compositions with iron oxide content between 52.0 and 53.0 mol% were made using high purity materials, 100% calcining and wet-ball milling for 18 and 36 hours. $\mu_o Q$-products of 500,000 were obtained in some instances with these materials; the average values for the series being approximately 10% higher than for those materials described in Report No. 53. In regard to temperature stability, no significant improvement was noted.

Disaccommodation

The study on the disaccommodation behavior of MF-8400-1, 2, 3, 8401-1, 2, 3, 8402-1, 2, 3 and MF-4373-A was continued. A new measuring technique was devised to allow the determination of disaccommodation at relatively short times; i.e., from 0.1 msec. to 500 seconds. During this time interval the disaccommodation behavior was studied at temperature levels of 0, 30, 60, 90 and 120°C. Also measurements extending to two weeks were made at room temperature. The study is incomplete, but preliminary conclusions are that disaccommodation: 1) is temperature dependent, 2) is minimized at iron oxide contents around 53 mol%, 3) is influenced to a certain extent by a decreasing Mn-Zn ratio, and 4) can be described by a logarithmic function with one or more relaxation constants.

SECTION B

Investigation of the Effects of Particle and Grain Size on $\mu_o Q$, Temperature Coefficient and Disaccommodation of Ni-Zn Ferrites.

Two compositions with iron oxide content near 53 mol% and a Mn-Zn ratio held constant at 1.94 were prepared. After calcining, the materials were wet ball-milled for periods of 2, 4, 8, 16 32 and 64 hours. The purpose of this milling procedure is to yield powders of varying fineness so that the influence of fired grain size on the magnetic properties of the material can be studied. The average powder particle size was determined by x-ray diffraction for each of these milling times. Coercive force measurements on the powders were also made. Toroidal samples were pressed and fired, and μ_o and Q values

were measured at frequencies of 100, 200, 400 800 and 1600 kc/s. The data indicate an improvement in the frequency stability of these materials with longer milling. The fired grain size of these materials will be determined for the next report and correlated with μ_o, Q, disaccommodation behavior and temperature coefficient.

PART II NICKEL-ZINC FERRITES

SECTION B

Investigation of the Effects of Particle and Grain Size on $\mu_o Q$, Temperature Coefficient and Disaccommodation of Ni-Zn Ferrites

Two compositions were prepared for this study; the basic Q-1 formula minus cobalt and, a stoichiometric Fe_2O_3 material with the same Ni-Zn ratio as Q-1. These materials were calcined at two different temperatures and wet ball-milled for periods of 2, 4, 8, 16, 32 and 64 hours. The purpose of this milling procedure is to yield powders of varying fineness so that the influence of fired grain size on the magnetic properties of the material can be studied. Particle size, as determined by x-ray diffraction and coercive force measurements, were made on the powders. Toroids were pressed and fired at varying temperatures. No magnetic data is available for this report. Measurements of μ_o and Q in the frequency range 100 kc/s to 500 mc/s are being made.

FOREWORD

GENERAL

In the past quarter we have changed somewhat the way of our approach to produce and study high quality ferrite materials. In this forword we will explain the reasons for this different approach and also the newly introduced measuring methods.

In accordance with these changes, we have had to alter slightly the system of reporting starting with this report. All results on Mn-Zn ferrite material and components will be reported in Part I, while Part II will be reserved for Ni-Zn ferrites.

Since there are some results to be reported yet which were gained on materials made in the past or on present production materials, each of these two parts will be split into a Section A and a Section B. Section A shall be used for continued studies on older materials using previous methods, while Section B will be reserved for work done using the new way of approach entirely.

The basic ideas of our present studies to be reported under Section B are the following:

Most of the materials developed so far for applications in the frequency range from 50 kc/s up to 250 mc/s were originated many years ago. At that time the basic requirement was high $\mu_o Q$-product over a given frequency range. Only in the last two years have the problems of temperature stability and disaccommodation become more evident and as a result limits on these effects have been established as a part of the technical requirements. By means of slight changes in composition and substantial improvement in the firing technique, some materials have been developed which have improved temperature behavior as well as satisfactory $\mu_o Q$-products. However, in many instances their disaccommodation behavior was worse than that of the older types of less temperature-stable materials. Since, on the basis of composition and firing techniques along, one was not able to relate μ_o, Q, T_k and disaccommodation as well, the art still remains today very much empirical. There is no doubt that basic parameters like saturation magnetization, crystalline anisotropy, magnetostriction and exchange-energy can be influenced by changes in composition which include, in the case of ferrites, the oxygen content. However, it is a well known fact that properties, e.g., like coercive force and permeability can be changed more drastically by means of changing the grain structure. For quite a number of materials, it has already been proven that the intrinsic coercive force can be varied by more than three orders of magnitude depending on whether a very fine grain powder or a

coarse crystalline material is used, e.g., in pure iron powder of single domain size a coercivity of greater than 1000 oersteds has been measured while in a dense polycrystalline state values of less than 0.1 oersteds have been measured. It is usually believed that the high coercive force obtained in powder with critical particle size can be observed only with relatively low density materials. However, there are quite a number of examples already proving that even in materials with more than 90% density, changing grain size can cause changes of coercivity of an order of magnitude or more. *

Since polycrystalline ferrites are usually produced with ceramic sintering methods, there is an obvious way of changing crystalline size by changing firing temperature and time. The same factors unfortunately also change the oxygen content of the material.

It was our first concern to use some technique which would permit us to establish the grain size first and later influence the oxygen content independently. Preliminary studies have shown that this can be done by first making a short firing in the temperature range between 1150 and 1500°C followed by a longer period of annealing at temperatures below 1000°C under controlled atmospheric conditions.

A second problem in manufacturing polycrystalline ferrites concerns the fact that a decrease in crystal size is usually accompanied by a change in density. We have learned in the past years that even this problem can be overcome fairly simply. If a very fine crystalline but dense material is desired, one has to start with very intensively milled and therefore highly reactive powders.

In order to obtain results which were reproducible, we had to know the average fineness of the powders used for pressing our test samples. We thus introduced the method of powder particle size determination by means of broadening of x-ray diffraction lines. We also use as a fairly reliable relative method, the measurement of the intrinsic coercive force. Both methods are discussed later in this section. As a rule we also work with well calcined materials in order that we may assume that the powder used for pressing is to a high degree a ferrite rather than a mixture of the various oxide components. In the latter case, the reactivity and, therefore, the final grain size obtained after firing, are highly dependent on the actual raw materials used.

*Schwabe & Campbell - Influence of Grain Size on the Square-Loop Properties of Lithium Ferrite - JAP Supp., March, 1963.

During the next three quarters we hope, by using the general preparative procedures outlined above and by evaluating our samples not only with respect to their magnetic properties but also by determining their grain size, to find a more complete understanding of the basic relations between magnetic properties. This is of considerable importance for applications in the military field since the proper selection of a material for highly specialized application is only poissible if one knows the relation between various properties and can therefore find the best compromise.

One particular problem we will be concern with is the relation between T_k and disaccommodation. There are various indications that the effects we are using to obtain a flat μ_o versus temperature relation and the undesired disaccommodation are of the same nature. This would mean that a certain amount of disaccommodation will always be found in a temperature-stable material. In order to observe disaccommodation effects better, a wider time range was desirable than previously used. We are currently using a new device which already permits the observation of permeability .002 secs. after normalization rather than after one minute which the previous method allowed. Details of this device are also explained below.

X-RAY PARTICLE SIZE DETERMINATION

Average powder particle size is determined through x-ray diffraction line broadening techniques. No effort is made to determine the distribution of particle sizes.

Broadening of x-ray line profiles may be attributed to two factors. First, broadening may be attributed to small particle size, and is related to the particle size by the Scherrer equation:

$$1) \quad B_{ps} = \frac{k \lambda}{t \cos \theta}$$

where B_{ps} = breadth due to particle size (in radians)

k = a constant, ranging from 0.7 to 1.7, but averaging about 0.9 and primarily dependent upon particle shape, the HKL of the reflecting plane, and method of measurement of line width.

λ = wavelength of incident x-radiation (in angstroms)

t = average particle diameter (in angstroms)

θ = Bragg angle

Second, additional line broadening may be attributed to lattice distortion by the equation:

$$2) \quad B_D = \sqrt{\frac{\Delta D}{D}} \tan \theta$$

where B_D = breadth due to fractional variation in plane spacings (in radians)

$\Delta D/D$ = fractional variation of lattice spacings

θ = Bragg angle

In addition to these two factors, there is an inherent line width which is the result of the geometry of the diffractometer and the x-ray tube target and divergence of the radiation. Therefore, any measurement of line width will include breadth due to these three factors. This inherent line breadth was determined for our equipment, through the use of a silicon standard. A graph of inherent line breadth versus θ was determined.

Line breadth is measured by manually turning to the required Bragg angles and making a fixed count or fixed time determination at that angle, insuring enough counts for a good statistical average. These points are then plotted as intensity versus Bragg angle and the half-height breadth is measured and converted to radians. Reflections which are primarily used are the 111, 220, 311, 400, 511 and 440.

If we let this initial breadth be B_{mo} and the inherent line breadth be B_s, then:

$$3) \quad B_m^2 = B_{mo}^2 - B_s^2$$

where B_m is the line breadth due only to particle size and distortion. However, the B_m curve is a combination of the $K\alpha_1$ and $K\alpha_2$ reflections. The $K\alpha_1$ line breadth may be separated by using the Jones method which assumes lines of a known profile (Gaussian, in this case). Therefore, the line breadth of a $K\alpha_1$ curve, consisting of breadth due to distortion and particle size is B.

$$4) \quad B^2 = B_{ps}^2 + B_D^2$$

$$\text{or: } 4a) \quad B^2 = \frac{(k\lambda)^2}{(t \cos \theta)^2} + \frac{\Delta D}{D} \tan^2 \theta$$

$$\text{and } 5) \quad B^2 \cos^2 \theta = \frac{(k\lambda)^2}{t^2} + \frac{\Delta D}{D} \sin^2 \theta$$

If a graph is plotted for values of $B^2 \cos^2 \theta$ (for the various reflections) versus $\sin^2 \theta$, with corrections made in the value of k for the various HKL's, the result will be a straight line which may be extrapolated to $\sin^2 \theta = 0$. The value at which the line crosses the $B^2 \cos^2 \theta$ axis is B_{ps}^2 and the particle size is then:

$$t = \frac{.9}{\sqrt{B_{ps}^2}}$$

$\Delta D/D$, then, is merely the slope of the straight line.

This method has an estimated accuracy of $\pm$ 5% under 600 Å, $\pm$ 10% for powder particle sizes under 1000 Å and 15% for powder particle sizes under 2000 Å.

Accuracy of measurement of lattice spacing variation is estimated at $\pm$ 5%, in any case.

INTRINSIC COERCIVE FORCE MEASUREMENTS

Coercive force is measured by what may be termed a "null" method. Refer to Fig. I.

The sample, in powder form, is enclosed in a glass ampule and inserted by means of a rod into the center of the pickup coil C_p, which itself is placed concentrically in the larger coil C_m. The switch S_1 is put into the saturate position and a 210 volt, 7 ampere input is applied through points 1 and 2 to the coil C_m for a brief period. The sample is now saturated. The coil is constructed so as to apply a field of 400 oersteds per ampere to the sample. This field is determined by the number of turns and length of the coil. Switch S_1 is now put into the measuring position. A demagnetizing current, which depends on the setting of the power supply, flows through the coil, C_m, in the direction opposite to the saturating current.

The meter, M_2, is calibrated to read directly in oersteds. Now the rod which holds the glass ampule is moved about the center position of the concentric coils C_p and C_m. If there is magnetization in the powder sample, there will be a change of flux in the pickup coil C_p which is observed on a ballistic galvanometer. This change of flux will be indicated by a ballistic deflection of the galvanometer. The demagnetizing current is increased until no deflection is observed at the galvanometer while displacing the sample and the coercive force is then read directly on meter M_2.

Circuit Diagram - Intrinsic Coercive Force Measurement

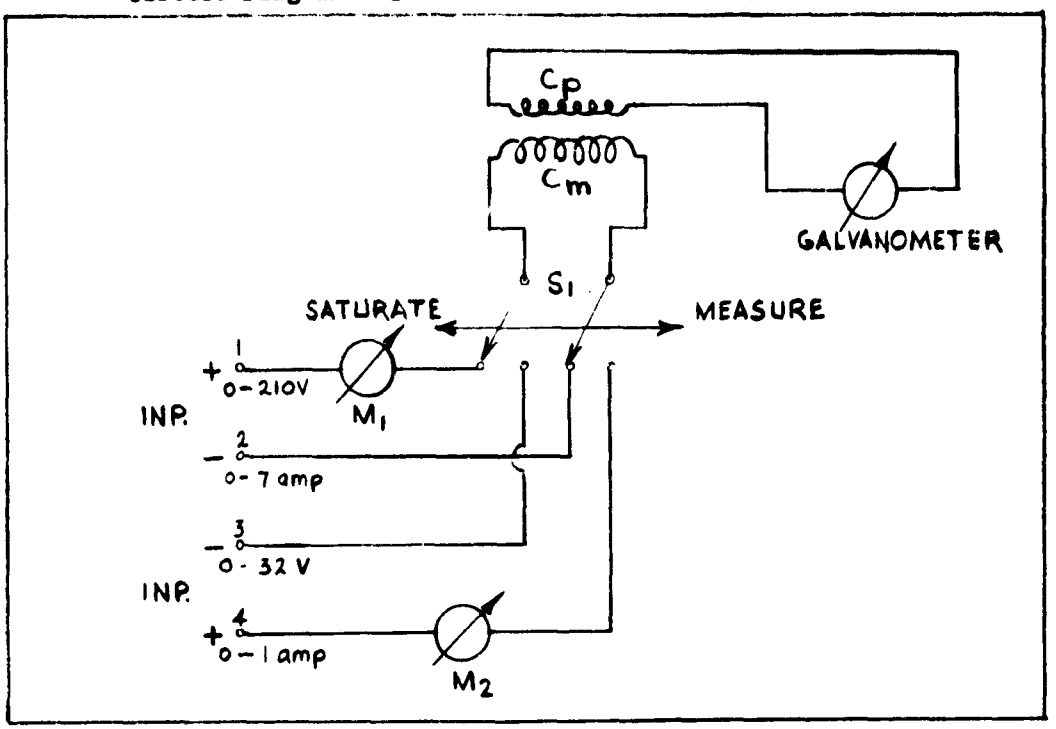

FIG. 1

SHORT TIME DISACCOMMODATION MEASUREMENT

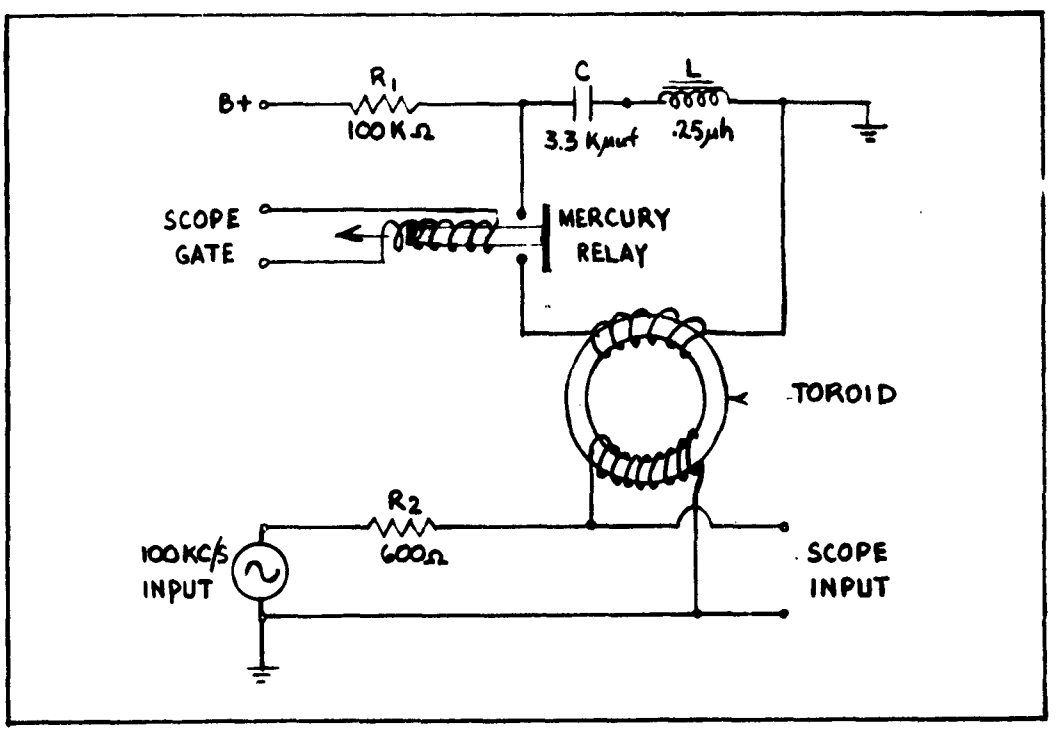

FIG. 2

Circuit Design - Disaccommodation Measurement

SHORT TIME DISACCOMMODATION MEASUREMENT

An oscillating circuit consists of a capacitance C, inductance L and the sample toroid in series with the contact of a mercury wetted relay. The contact of the relay is normally open. The coil of the relay is energized during the retrace of a Tektronix oscilloscope through a special gate output provided in the scope. When the relay contact is open the capacitance C becomes slowly charged through the resistor R . During the retrace of the scope the contact closes, thus discharging capacitance C. This sets up an oscillation of 200 kc frequency. This is a damped oscillation with a time constant of 30 μsec. This damped oscillation demagnetizes the ferrite toroid.

A low amplitude 100 kc signal is continuously applied through a 600 ohm resistor R to the secondary winding on the toroid. The voltage drop across the secondary winding is measured on the scope of the Tektronix oscilloscope. The amplitude of the signal is proportional to the impedance of the secondary winding on the toroid, since the impedance itself is kept small in comparison to the 600 ohm resistance. This impedance is a function of the permeability of the ferrite material. In short, as the ferrite disaccommodates and the permeability changes, the impedance of this circuit element changes and the amplitude of the signal read on the oscilloscope changes. The ratio of the amplitude, after a selected period of time, to the initial amplitude is the measurement taken.

The repetition rate of the demagnetization can be varied between 50 times per second and .02 times per second, using different sweep time settings on the oscilloscope. The shortest time at which a permeability measurement can be made is 0.1 msec.

PART I - Mn-Zn FERRITES

SECTION A.

HIGH PURITY MATERIALS IN RELATION TO TEMPERATURE STABILITY AND $\mu_o Q$ PRODUCT

In Report No. 53, pages 7-8, Tables 270-271, Graphs 578 to 580, results were presented on materials containing 50% by weight of well pre-reacted calcines of the same composition and covering materials calculated on the basis of from 52.5 to 53.5 mol% iron oxide.

It was found that the introduction of the calcines into the materials resulted in noticeably improved $\mu_o Q$ values, without appreciably affecting the change of μ_o vs. temperature. Best over-all results were reported on materials calculated on the basis of slightly less than 53.0 mol% iron oxide.

In continuing this investigation, it was decided to initiate a new series of materials, based on similar iron oxide ratios, but embodying the following variants of preparation:

1. Use of high-purity materials.
2. 100% pre-calcination (in air) of the pre-mixed batches at two different peak temperatures: 2000°F and 2300°F, respectively.
3. Wet ball-milling the materials for two different periods: 18 hours and 36 hours.

At the same time, it was planned to determine by chemical analysis, the gain in iron oxide due to milling, and thereby arrive at the actual values of the iron oxide ratios as present in the specimen tested.

The new test series, MF-8649, was based on three compositions in the range of iron oxide ratios that had proven as critical in previous investigations (52.0 to 53.0 mol%).

In order to maintain similar Curie points for the three compositions, the zinc oxide was adjusted in the same ratio with increasing iron oxide.

The composition of MF-8649, as calculated in mol%, is:

MF-8649	-1	-2	-3
Fe_2O_3	52.0	52.5	53.0
MnO	32.0	31.0	30.0
ZnO	16.0	16.5	17.0

(*)
The iron oxide used was a commercially produced material of exceptional purity. The manganous oxide was obtained from reagent grade manganous carbonate of 99.9% purity and containing only traces of SiO_2. The zinc oxide was of good commercial purity (99.9% ZnO).

PREPARATION OF MATERIALS

The three compositions were wet-milled for three hours, dried and granulated. One half of each material was calcined (in air) to approximately 2000°F, the other half to approximately 2300°F. Of these calcines, one half was wet ball-milled for 18 hours, the other half for 36 hours, and all materials were dried.

Based on the three compositions and on the two different procedures each in calcining and in milling, a total of twelve materials resulted.

Table 275 (a) contains the system of identification used for the whole group, together with the gain in iron oxides due to milling, as obtained by gravimetric analysis (cupferron method).

All materials were re-milled wet for a few minutes, with the addition of organic binders, and spray-dried.

Toroids (approximately 25 mm o.d. before firing) were pressed and complete sets of the whole series were fired in batch type kilns to different peak temperatures, combined with cooling in nitrogen. Table 275 (b) gives a schedule of the type of firings used.

Data on μ_o, Q and $\mu_o Q$-products obtained on five of these firings and measured at frequencies of 100, 200 and 300 kc/s, are given in Tables 276 to 278.

Values of μ_o vs. temperature (-65°C to +150°C), measured at 100 kc/s, are presented in Graphs 593 to 601, for three different firings.

From the data presented, the following conclusions may be drawn:

* Total impurities 0.1%, including .01% of SiO_2, as compared with average of high-grade iron oxides containing approximately .2% total impurities, including .02 to .04% of SiO_2.

Table 275 (a)

The iron oxide gained in milling two different calcines for two different periods was determined by gravimetric analysis and found to be the same for both calcines, namely approximately 0.5 mol% Fe_2O_3 for the 18-hour milling, and approximately 0.75 mol% Fe_2O_3 for the 36-hour milling.

Apparently, the considerable difference in hardness between a 2000°F and a 2300°F calcine had very little effect on this result, and the smaller than expected gain of 0.25 mol% Fe_2O_3 at the 36-hour milling over the 18-hour milling, can be explained by the cushioning effect of increasing viscosity on prolonged milling.

Table 276 to 278

Generally, the effect of the variations in calcining and milling techniques as used in this investigation is not very startling. However, when considering this conclusion in light of the work presented in Section B, two factors shall be pointed out. 1) No provision was made in this work to reduce or prevent reoxidation of the calcine during the cooling cycle. Thus an inhomogeneous powder containing a hematite phase was prepared and used. 2) During the milling a charge 2-1/2 times greater was used and the percent increase in Fe_2O_3 was less than in the work reported in Section B. A μ_oQ-product of 440×10^3 (100 kc/s) was the best average of the five firings reported and was obtained with material MF-8649-2, preparation "A" (100% calcined at 2000°F and wet-milled for 18-hours). This material was calculated on the basis of 52.5 mol% Fe_2O_3, and contained actually 53.0 mol% Fe_2O_3, after milling.

Next best average μ_oQ-product of 410×10^3 was obtained with MF-8649-2, preparation "D" (100% calcined at 2300°F, milled for 36-hours and actually contained 53.2 mol% Fe_2O_3)

Considering the two materials, MF-8649-1 and MF-8649-2, it appears that the 36-hour milling was advantageous only when the materials consisted of high-fired and less reactive calcines. This, however, also increased the actual iron oxide ratios of the material to 53.2 mol%.

When measuring at a frequency above 100 kc/s, μ_o increases slightly and Q decreases sharply. At 300 kc/s, only about 40% of the μ_oQ-product measured at 100 kc/s, remains with the materials low in iron oxide. This proportion is slightly better (to about 50%), with materials containing higher iron ratios.

Summarizing, it was established that the use of high-purity materials, combined with proper calcination, milling and adjustment of the actual iron oxide ratio to approximately 53 mol%, yielded μ_oQ-products up to and above 500×10^3 (at 100 kc/s) in some firings. The average results of this work are considered as very satisfactory and above the average of previous work.

Graphs 593 to 601

The change of $\Delta\mu_o/\mu_o$ vs. temperature in the range of -65°C to +150°C is presented as obtained from three different firings.

Each graph depicts one basic composition and the effect upon $\Delta\mu_o/\mu_o$ vs. temperature, of variations in preparation (see Table 275) which at the same time cause changes in the actual iron oxide ratios of the material.

In examining these graphs, the relation of iron oxide ratios with the type of firing technique used becomes apparent. With firing to the relatively high peak temperature of 2480°F (Graphs 593 to 595) best results were obtained with preparation "B" (52.74 mol% Fe_2O_3, actual). The same material, of preparation "D", shows a slightly irregular performance between 0°C and 85°C. All materials above 53 mol% Fe_2O_3 show marked irregularities in the low temperature range.

With firing No. 2, (Graphs 596 to 598) to a peak temperature of 2400°F, MF-8649-2 preparation "A", (53.0 mol% Fe_2O_3, actual) gave the best result.

In firing No. 3, (Graphs 599 to 601) to a slightly lower peak temperature of 2380°F, good temperature coefficients were obtained on a number of materials, with low $\Delta\mu/\mu^2\Delta T$ over the whole temperature range for materials containing 53.0 to 53.5 mol% Fe_2O_3. Above 53.5 mol% Fe_2O_3, one material, MF-8649-3, preparation "B", resulted in the lowest temperature coefficient of the whole series.

In summary, it is evident that best temperature coefficients are obtained with materials based on actual iron oxide ratios of from 52.75 to 53.5 mol%, the lower mol-ratios are better suited for higher firing temperatures and the higher mol-ratios are better suited for lower firing temperatures.

Generally, in the use of high-purity materials, no significantly different effect with the performance of $\Delta\mu_o/\mu_o$ vs. temperature was observed, as compared with materials of average commercial purity.

DISACCOMMODATION (AGING) OF Mn-Zn FERRITES

The investigation initially reported on in Report No. 52, page 10, has been extended so as to include in this report data on disaccommodation at varying temperatures and at times ranging from 0.1 μsec. to seven weeks. The materials studied are the same as those described in Report No. 52; the same toroids were used for the measurements. The technique as described in the foreword was used for measurements in the time range .0001-500 seconds. The measurements in the time range one minute to seven weeks were made on a General Radio Inductance Bridge. All measurements were made at a frequency of 100 kc/s.

Graphs 602, 603 and 604 show the percent change in permeability versus disaccommodation time for temperature levels of 0, 30, 60, 90 and 120°C. The measurements were taken at .0001, .002, .010, .040, .080, .80, 8.0, 100 and 500 seconds. The percent change in permeability is calculated on the basis of the permeability at .0001 seconds.

The data is not yet complete. What is lacking are measurements at the various temperature levels mentioned above for disaccommodation times up to at least a week. This data will be obtained for the next report. Graph 605 shows the complete range of measurements to aging times of seven weeks for the temperature level 25°C for the materials MF-8400, 8401, 8402 and is an example of what will be obtained at the other temperature levels for the next report.

Graphs 606 and 607 describe the same type of data as Graphs 602-605 for MF-4373-A. Disaccommodation data on this material was first presented in Report No. 53. MF-4373-A is of interest in this study as it shows significant disaccommodation at relatively short times already. It is of interest to discover if disaccommodation approaches a final equilibrium value and if so what that value is; and further to discover if this value is temperature dependent. This material promises to be of use in determining the maximum effect of disaccommodation.

On the basis of data thus far accumulated, it appears evident that disaccommodation can be described by a logarithmic function and that this function contains one or more relaxation constants which are temperature dependent. This is in agreement with results reported in the literature, e.g., Smit and Wijn, "Ferrites". Determining the final equilibrium value of disaccommodation will aid considerably in discovering this logarithmic function. On the basis of this function, perhaps a reasonable hypothesis on the nature of disaccommodation can be generated and from this an effective approach to further experimentation.

The data also appears to show that disaccommodation is related to excess iron. A minimum effect tends to be observed at a value of approximately 53 mol% Fe_2O_3. This is seen in the Graphs 602, 603 and 604. These graphs also show that with a constant value of Fe_2O_3 in these materials the disaccommodation decreases somewhat with a decreasing Mn-Zn ratio. These two observations strongly suggest that disaccommodation is related to the variable valence states of iron and manganese.

SECTION B

INVESTIGATION OF THE EFFECTS OF PARTICLE AND GRAIN SIZE ON $\mu_o Q$, TEMPERATURE COEFFICIENT AND DISACCOMMODATION OF Mn-Zn FERRITES

Initial compositions near 53 mol% Fe_2O_3 were chosen for this investigation, since best results were obtained previously in this area of composition. The MnO-ZnO ratio was held constant at 1.94. The compositions used were as follows:

MOL%	8644-1	8644-4
Fe_2O_3	52.5	53.3
MnO	31.3	30.8
ZnO	16.2	15.9

The mixes, using raw materials of commercial purity, were wet-milled, dried, screened and calcined.

The material was calcined in a laboratory batch kiln following the general procedure developed for firing telecommunication parts. It was heated to 2225°F, held there for two hours, dropped to 2000°F, nitrogen introduced, held at this temperature for two hours and cooled in nitrogen.

A milling test series was then run on this material. The test was run with small ball mills containing a charge of 5 kilograms of 5/8" steel balls, 210 grams material and 420 cc water. Samples were drawn from these mills at intervals of 2, 4, 8, 16, 32 and 64 hours. Coercive force measurements were taken on these samples. Graph 608 shows coercive force versus milling time for these materials. The average powder particle size was determined using x-ray diffraction line broadening technique as described earlier in this report. Graph 609 shows coercive force versus average powder particle size for this material.

After completion of the milling series, batches were made for each of the milling periods, 2, 4, 8, 16, 32 and 64 hours using the same charge ratio used in the milling test: 210 grams material, 420 cc water and 5 kilograms of 5/8" steel balls. After milling, approximately three weight percent of methocel dissolved in alcohol was mixed with the batches. The batches were then dried, milled, screened and toroids of 7 mm o.d. pressed.

The toroids were heated to 600°F to burn out the binder. Firings were accomplished using a battery of platinum wound tube kilns. Toroids to be fired were placed in a platinum sleeve inside the end of a mullite tube. The mullite tube was placed in a tube kiln at the desired peak temperature. After 10 minutes at peak temperature, the mullite tube was removed to a second tube kiln, held at 975°C in an atmosphere of nitrogen and cooled in nitrogen.

Measurements of density and fired grain size have been initiated and these will be presented in our next report along with measurements of the magnetic parameters. Initially μ_o and Q values have been obtained at 100, 200, 400, 800 and 1600 kc/s. Graphs 610 to 615 show the $\mu_o Q$-products versus frequency for each of the milling times. The permeabilities indicated on the graphs remain approximately constant over the frequency range tested; i.e., the change in the $\mu_o Q$-product is a result of the changing Q values. Some of the curves are plotted to show initial points at somewhat higher values than the measured values. These samples had high Q values and at lower frequencies, 100 kc/s, the magnetic losses in the material were so low that the resistance of the winding became a very significant factor in the measurement.

The data given in the graphs show a definite improvement in the frequency stability of these materials with longer milling. However, it would be premature at this time to make any positive statement about the exact cause of this phenomenon. There is a sizable increase in the iron content of these materials with increasing milling time. Wet chemical analysis of the two hour and sixty-four hour milled materials showed an increase of over 1.5 weight% Fe_2O_3 for the sixty-four hour milled materials. In these compositions, this represents an increase of close to two mol% Fe_2O_3. Material is being prepared with much lower initial Fe_2O_3 content in an attempt to determine how significant the increase in Fe_2O_3 content, due to milling, is in conjuction with grain size and density.

PART II - Ni-Zn FERRITES

SECTION A

No work has been done during this quarter to report in this section. Most of the work done previously in the frequency ranges 2-12 mc/s, 20-70 mc/s, 70-200 mc/s and 200-500 mc/s has reached the point where fresh experimental ideas are needed. These fresh experimental ideas are being formulated in the light of the new approach as discussed in the foreword and most of the future work in Ni-Zn will be reported in Section B.

We believe, that before any further significant improvements can be made in the properties of Ni-Zn ferrites which are to be used in the frequency ranges cited above, a basic study on the influence of grain size and the cause of time dependent effects is required. We expect, however, to continue some work on Ni-Zn materials along lines previously followed. In this regard, we hope to initiate, during the next quarter, a study on material MF-6835-3, for the frequency range 2-12 mc/s, using high purity materials. This study will be directed toward the objective of lowering the temperature coefficient of μ_o for this material.

SECTION B

INVESTIGATION OF THE EFFECTS OF PARTICLE AND GRAIN SIZE ON $\mu_o Q$, TEMPERATURE COEFFICIENT AND DISACCOMMODATION OF Ni-Zn FERRITES

In order to effectively study Ni-Zn ferrites for their application in the various frequency ranges prescribed in our contract, it is necessary to examine a material over the entire frequency spectrum rather than just a small portion of it. A material which shows poor properties in one area of the frequency spectrum may very well be useful in another area. After newly prepared materials are studied, they will be reported in our quarterly reports and the interesting ones will be discussed in regard to their usefulness in the various frequency ranges.

Of basic importance to our new approach on Ni-Zn ferrites, is the influence of grain size on permeability and Q. Thus, paralleling the investigation in Section B of Part I on Mn-Zn ferrites, an investigation is proceeding on Ni-Zn ferrites.

Two compositions have been chosen; one the basic Q-1 formula minus the cobalt addition, and the other a stoichiometric Fe_2O_3 composition with the same Ni-Zn ratio as Q-1. Cobalt has been specifically left out of these compositions in this initial study. The presence of cobalt in Ni-Zn materials causes them to disaccommodate considerably and it is desired to eliminate this complicating factor. The $\mu_o Q$-products are expected, therefore, to be less than heretofore presented for Ni-Zn ferrites.

The compositions are as follows:

	9000	9001	
Fe_2O_3	61.80	50.00	(mol%)
ZnO	22.15	28.98	"
NiO	16.05	21.02	"

The materials were calcined at two different temperatures, 2200°F and 2400°F, for two hours. The calcined materials were then milled for the following periods of time - 1 hour (dry), 2, 4, 8, 16, 32, 64 and 127 hours. After the first hour water was added. Coercive force and particle size measurements were made after each milling time and these results are shown in Graphs 616, 617 and 618. Particle size measurements for the 2200°F calcine have not been completed yet.

Milling times of 2, 8, 32 and 64 hours were selected for study. Some of these materials have been pressed into small toroids (.70 cm o.d.) and firings at various temperatures have begun. No data is yet available to present in this report. Measurements of the permeability in the frequency range 100 kc/s to 100 mc/s are being made.

PART III

RESEARCH PLANNED FOR NEXT QUARTER

1. High Purity Mn-Zn Ferrites - Three of the compositions with highest $\mu_o Q$ products reported in Part I of this report will be studied in parallel with three compositions prepared previously with commercial grade materials and which had high $\mu_o Q$-products. This study is expected to shed positive light on the significance of high purity materials. At the same time, the disaccommodation of these materials will be investigated.

2. The disaccommodation of MF-8400 -1, 2, 3, 8401 -1, 2, 3, 8402 - 1, 2, 3 and MF 4373-A will be studied further by extending the investigation presented in this report to longer times and higher temperatures.

3. The study on Mn-Zn ferrites presented in Section B of Part I will be continued. Density and fired grain size measurements will be reported. Disaccommodation and temperature stability will be investigated and the influence of annealing on these effects will be included.

4. An investigation will be conducted to further lower the temperature coefficient of nickel-zinc ferrite in the 2-12 mc/s range through the use of high purity materials.

5. The study on nickel-zinc ferrites presented in Section B of Part II will be continued. μ_o and Q values covering the frequency range from 100 kc/s to 500 mc/s will be measured and if time permits, grain size measurements will be made.

PART IV

MANHOURS SPENT ON CONTRACT FOR THE PERIOD 1 December 1962 to 28 February 1963

NAME	TITLE	HOURS
E. Schwabe	Physicist-Supervisor	216
K. Wetzel	Chemist	385
D. Sullivan	Ceramic Engineer	443
W. Stollar	Ceramic Engineer	272
C. O'Neill	Chemist	186-1/2
S. Golian	Ceramic Engineer	58
M. Eisenberg	Project Engineer	37
K. Sivak	Chemist	7
C. Cooper	Technician	11
P. Dacey	Technician	22-1/2
J. Holden	Technician	144
E. Hozeny	Technician	62
D. Kinsley	Technician	194
G. Lee	Technician	216
C. Lotz	Technician	57
E. Szatkowski	Technician	222
M. Zudonyi	Technician	2-1/2
S. Rubarski	Laboratory Assistant	106-1/2

GRAPH 593

FEBRUARY 1963

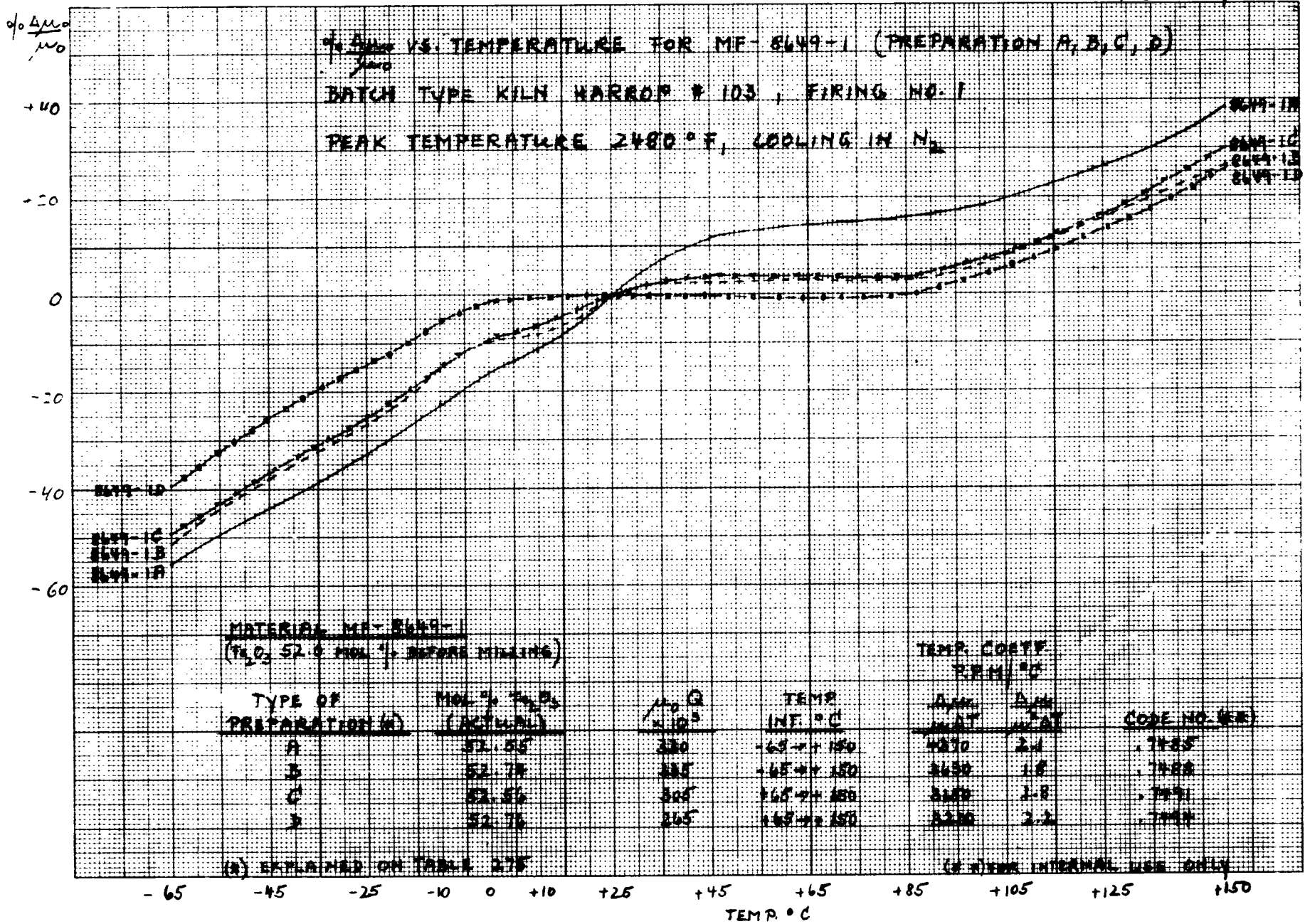

GRAPH 594

FEBRUARY 1963

% $\frac{\Delta\mu}{\mu}$ vs. TEMPERATURE FOR MF-8649-2 (PREPARATION A, B, C, D)

BATCH TYPE KILN HARROP # 103, FIRING NO. 1

PEAK TEMPERATURE 2480° F, COOLING IN N_2

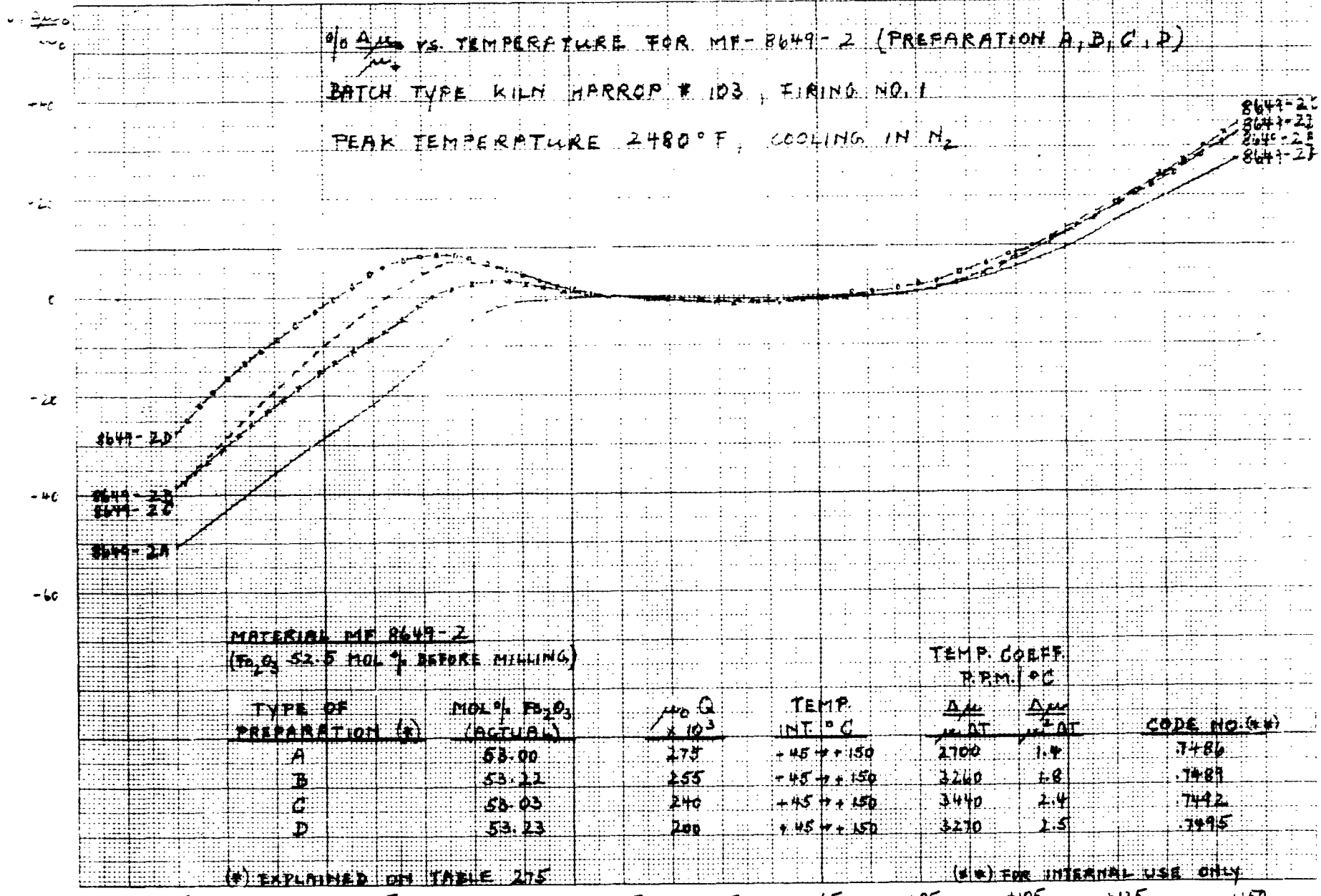

MATERIAL MF 8649-2

(Fe_2O_3 52.5 MOL % BEFORE MILLING)

TYPE OF PREPARATION (*)	MOL % Fe_2O_3 (ACTUAL)	$\mu_0 Q \times 10^3$	TEMP. INT. °C	TEMP. COEFF. P.P.M./°C $\frac{\Delta\mu}{\mu} \Delta T$	TEMP. COEFF. P.P.M./°C $\frac{\Delta\mu}{\mu^2} \Delta T$	CODE NO. (**)
A	53.00	275	+45 to +150	2700	1.4	7486
B	53.22	255	+45 to +150	3240	1.8	7489
C	53.03	240	+45 to +150	3440	2.4	7492
D	53.23	200	+45 to +150	3270	2.5	7495

(*) EXPLAINED ON TABLE 275

(**) FOR INTERNAL USE ONLY

GRAPH 595

FEBRUARY 1963

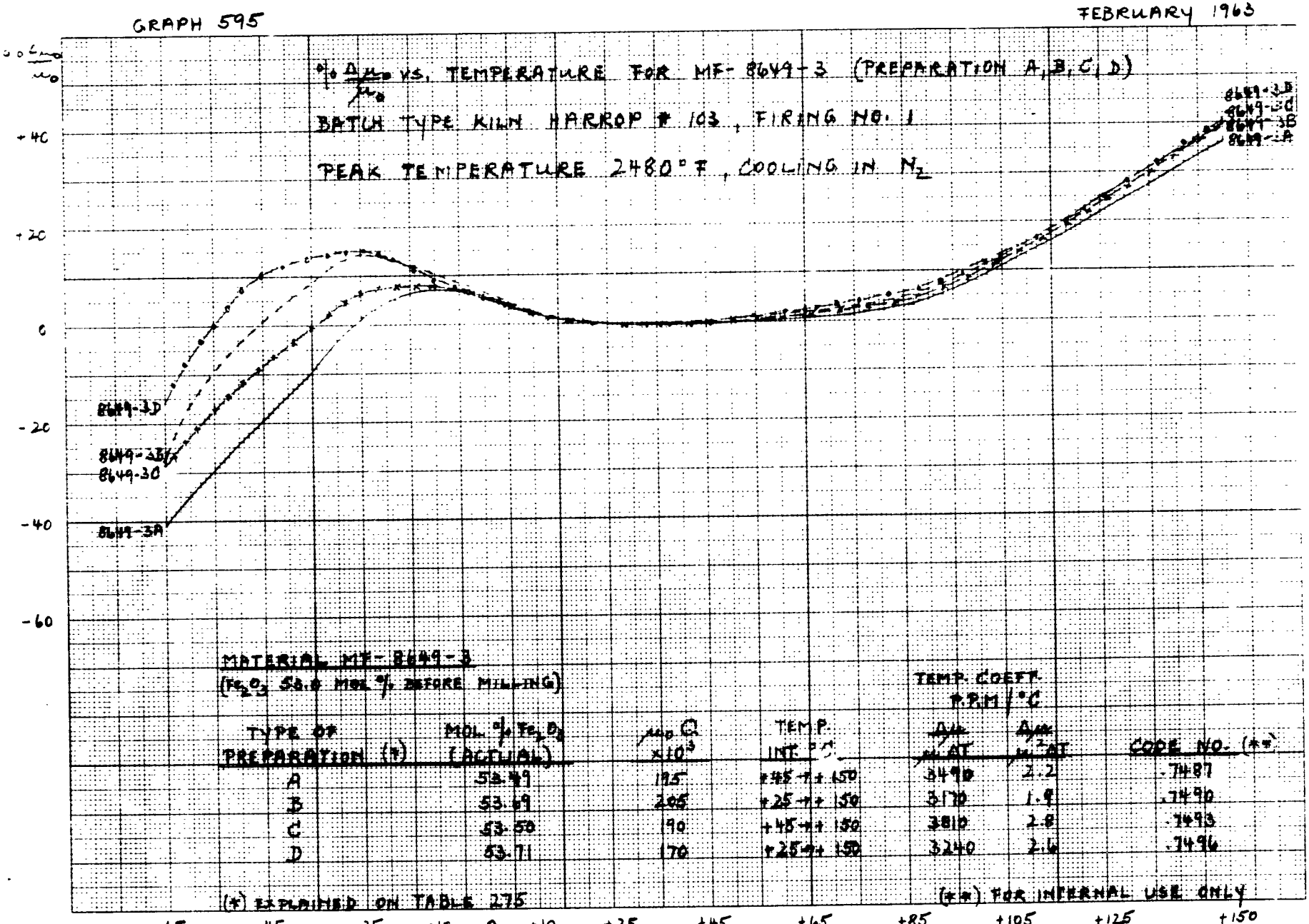

MATERIAL MF-8649-3
(Fe_2O_3 53.8 MOL % BEFORE MILLING)

TYPE OF PREPARATION (*)	MOL % Fe_2O_3 (ACTUAL)	$\mu_0 Q$ $\times 10^3$	TEMP. INT. °C	TEMP. COEFF. P.P.M./°C $\frac{\Delta\mu}{\mu}$ AT	$\frac{\Delta\mu}{\mu^2}$ AT	CODE NO. (**)
A	53.49	195	+45 TO +150	3490	2.2	.7487
B	53.69	205	+25 TO +150	3170	1.9	.7490
C	53.50	190	+45 TO +150	3810	2.8	.7493
D	53.71	170	+25 TO +150	3240	2.4	.7496

(*) EXPLAINED ON TABLE 275

(**) FOR INTERNAL USE ONLY

GRAPH 596

FEBRUARY 1963

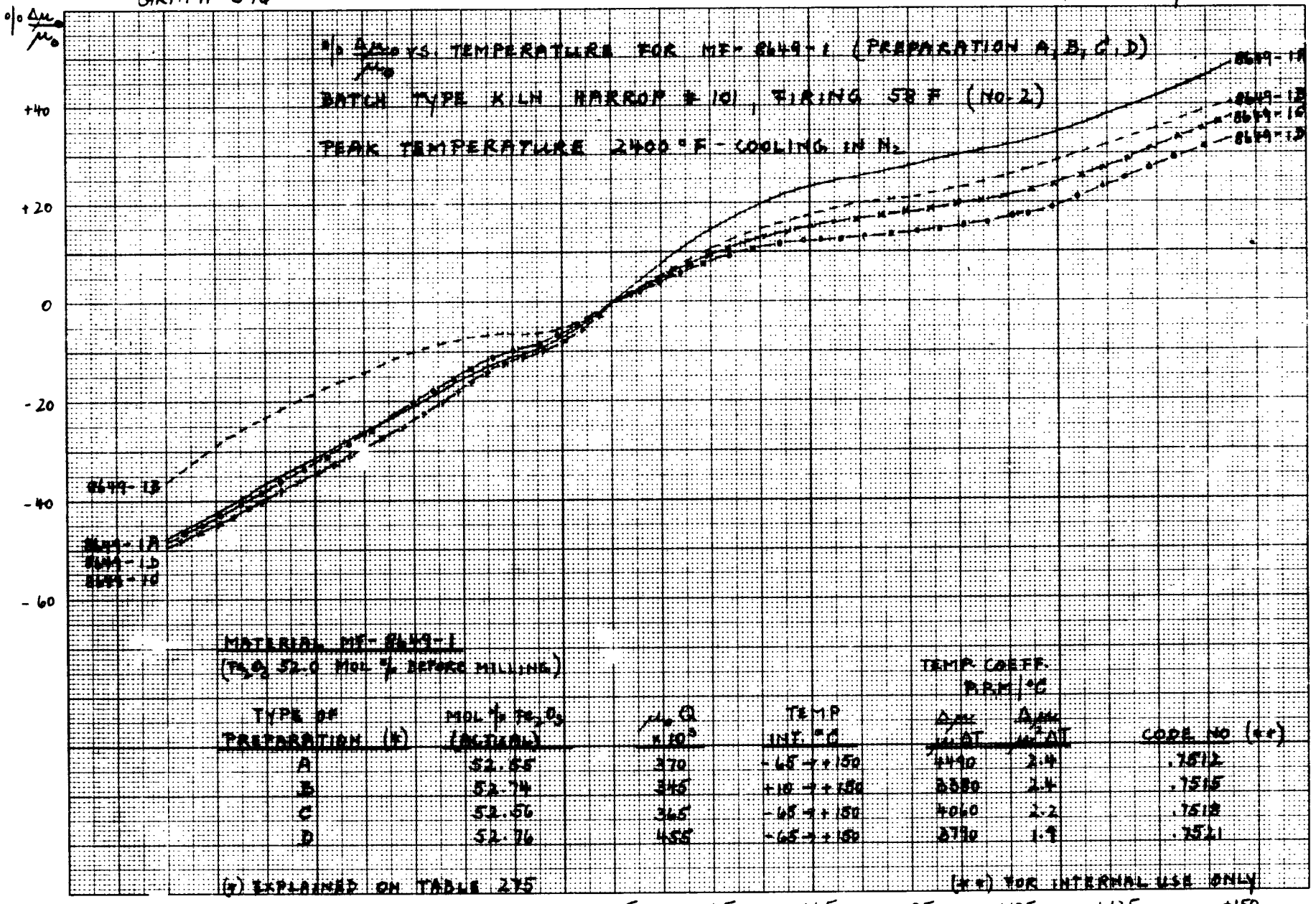

MATERIAL MF- 6649-1
(Ta_2O_5 52.0 Mol % BEFORE MILLING)

TYPE OF PREPARATION (#)	Mol % Fe_2O_3 (ANALYSIS)	μ_0 @ × 10³	TEMP INT. °C	TEMP. COEFF. P.P.M./°C $\frac{\Delta\mu/\mu_0}{\Delta T}$	$\frac{\Delta\mu/\mu_0}{\Delta T^2}$	CODE NO (**)
A	52.65	370	-65 → +150	4440	2.4	.7512
B	52.74	345	+10 → +150	3580	2.4	.7515
C	52.56	365	-65 → +150	4060	2.2	.7518
D	52.76	455	-65 → +150	3770	1.9	.7521

(#) EXPLAINED ON TABLE 275

(**) FOR INTERNAL USE ONLY

GRAPH 597

FEBRUARY 1963

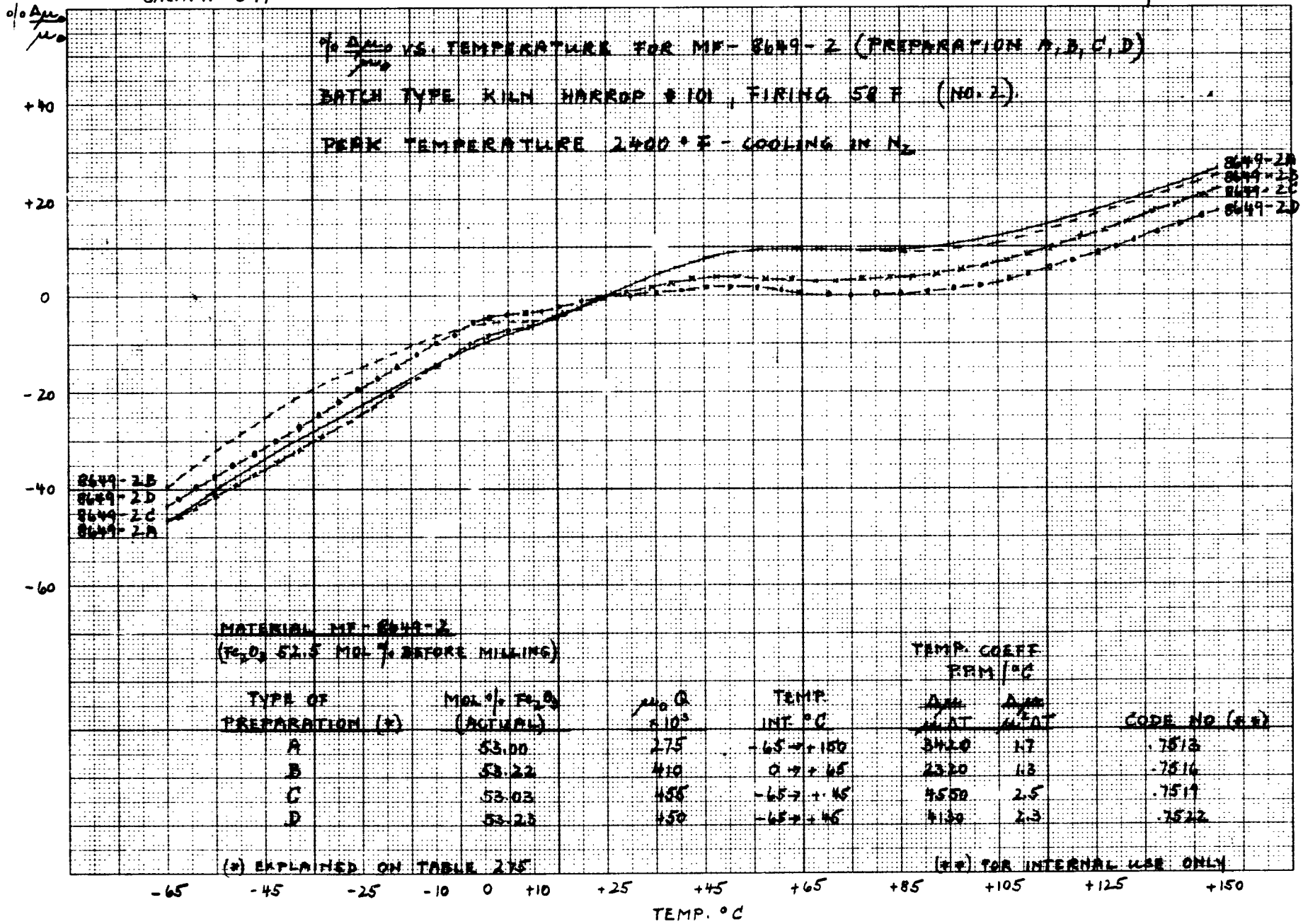

MATERIAL MF-8649-2

(Fe_2O_3 52.5 MOL % BEFORE MILLING)

TYPE OF PREPARATION (*)	MOL % Fe_2O_3 (ACTUAL)	$\mu_0 Q$ $\times 10^3$	TEMP. INT. °C	TEMP. COEFF PPM/°C $\frac{\Delta\mu}{\mu}$ AT	TEMP. COEFF PPM/°C $\frac{\Delta\mu}{\mu}$ AT	CODE NO (**)
A	53.00	275	-65 → +160	342.0	1.7	.7513
B	53.22	410	0 → +65	232.0	1.3	.7514
C	53.03	455	-65 → +45	455.0	2.5	.7517
D	53.25	450	-65 → +46	413.0	2.3	.7512

(*) EXPLAINED ON TABLE 275

(**) FOR INTERNAL USE ONLY

GRAPH 598

FEBRUARY 1963

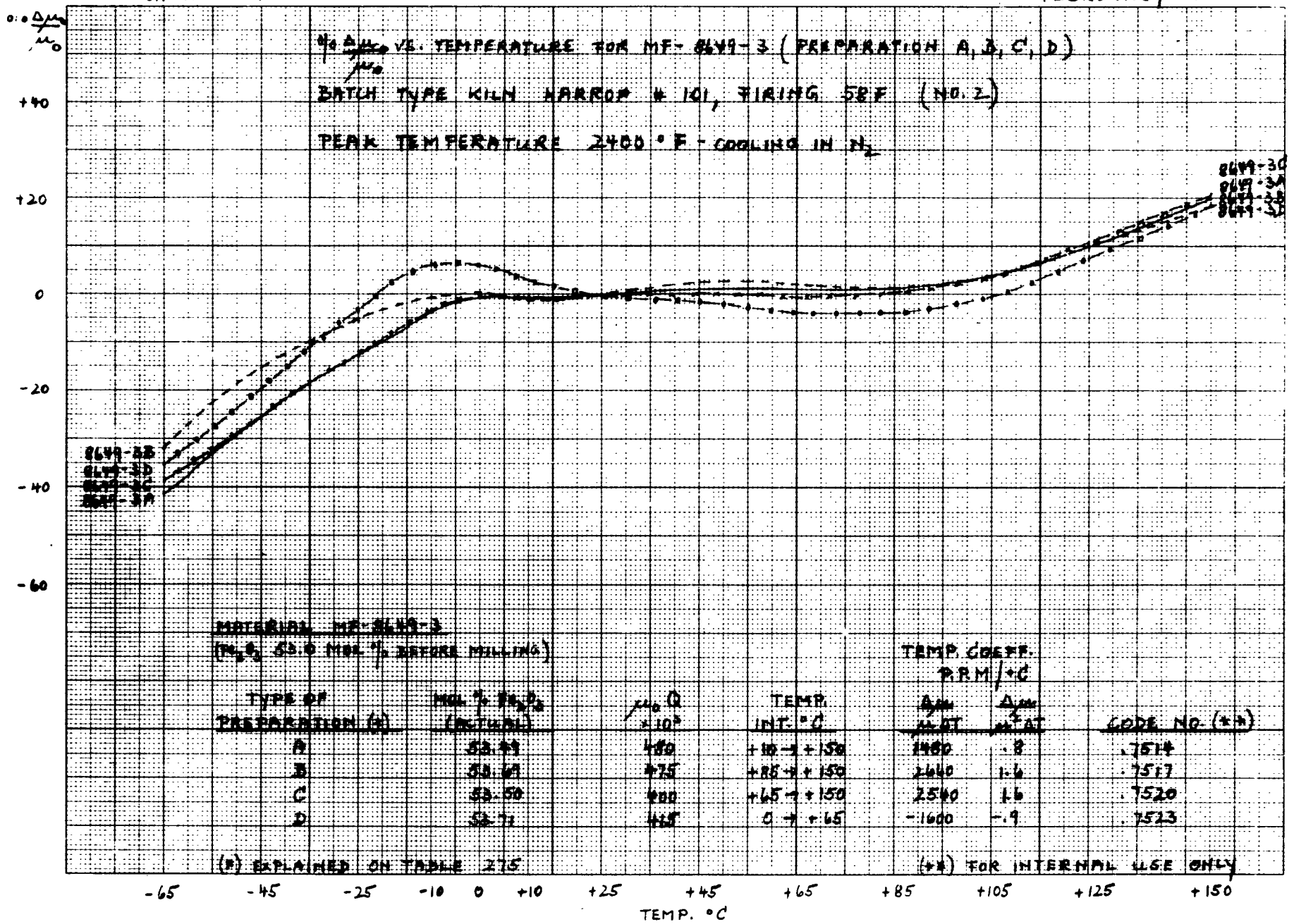

MATERIAL MF-8649-3
(Fe_2O_3 53.0 MOL % BEFORE MILLING)

TYPE OF PREPARATION (#)	MOL % Fe_2O_3 (ACTUAL)	$\mu_0 Q \times 10^3$	TEMP. INT. °C	TEMP. COEFF. PPM/°C $\frac{\Delta\mu}{\mu_0}$ AT	TEMP. COEFF. PPM/°C $\frac{\Delta\mu}{\mu_0^2}$ AT	CODE NO. (**)
A	52.99	480	+10 → +150	1480	.8	.7514
B	53.69	475	+85 → +150	2640	1.6	.7517
C	53.50	400	+65 → +150	2540	1.6	.7520
D	53.71	415	0 → +65	-1600	-.9	.7523

(#) EXPLAINED ON TABLE 275

(**) FOR INTERNAL USE ONLY

GRAPH 599

FEBRUARY 1963

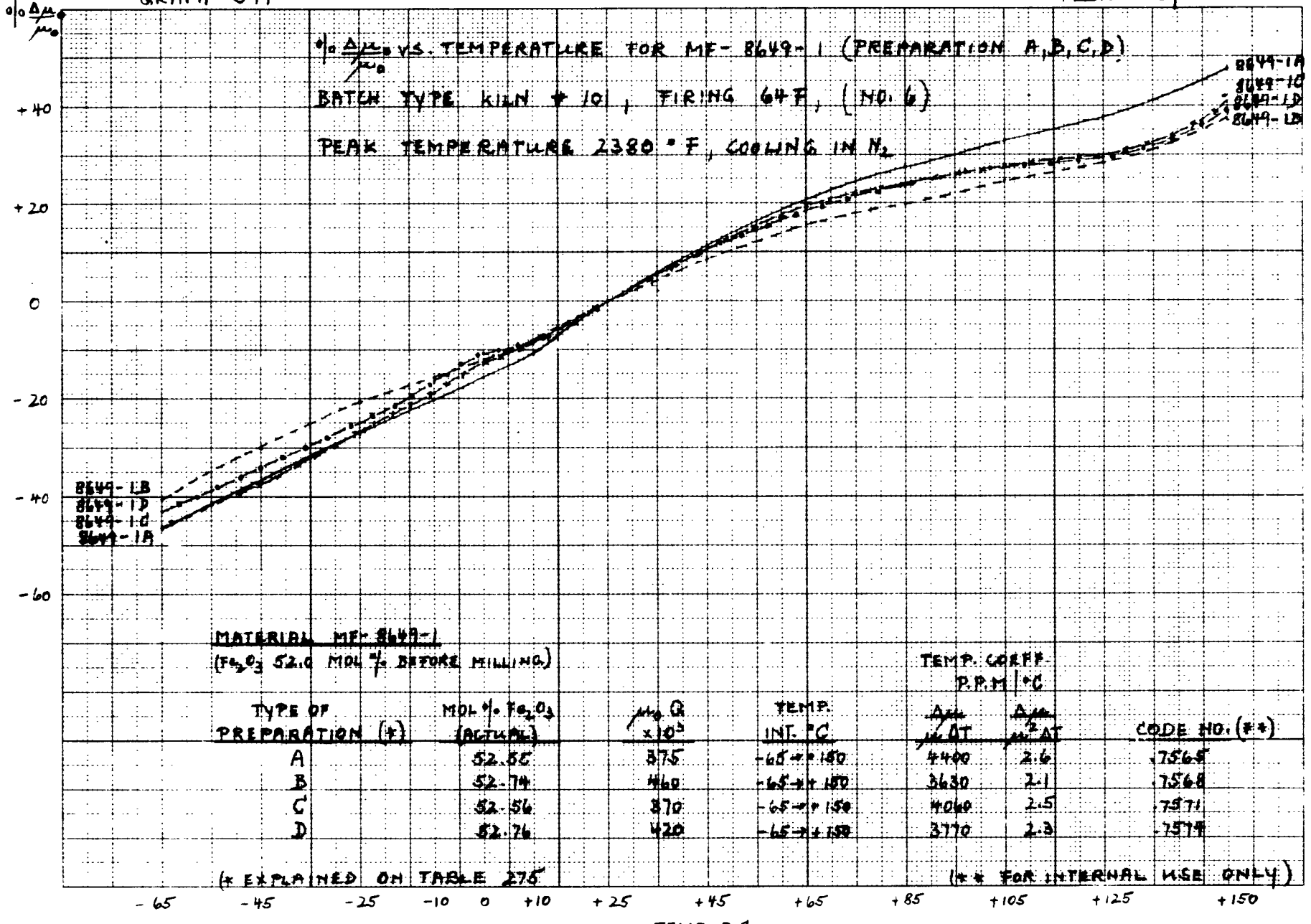

MATERIAL MF-8649-1
(Fe_2O_3 52.0 MOL % BEFORE MILLING)

TYPE OF PREPARATION (*)	MOL % Fe_2O_3 (ACTUAL)	$\mu_0 Q \times 10^3$	TEMP. INT. °C	TEMP. COEFF. P.P.M. / °C $\frac{\Delta\mu}{\mu_0 \Delta T}$	TEMP. COEFF. P.P.M. / °C $\frac{\Delta\mu}{\mu_0^2 \Delta T}$	CODE NO. (**)
A	52.55	375	-65 → +150	4400	2.6	7565
B	52.74	460	-65 → +150	3630	2.1	7566
C	52.56	370	-65 → +150	4060	2.5	7571
D	52.76	420	-65 → +150	3770	2.3	7574

(* EXPLAINED ON TABLE 275

(** FOR INTERNAL USE ONLY)

GRAPH 600

R. FRY 1963

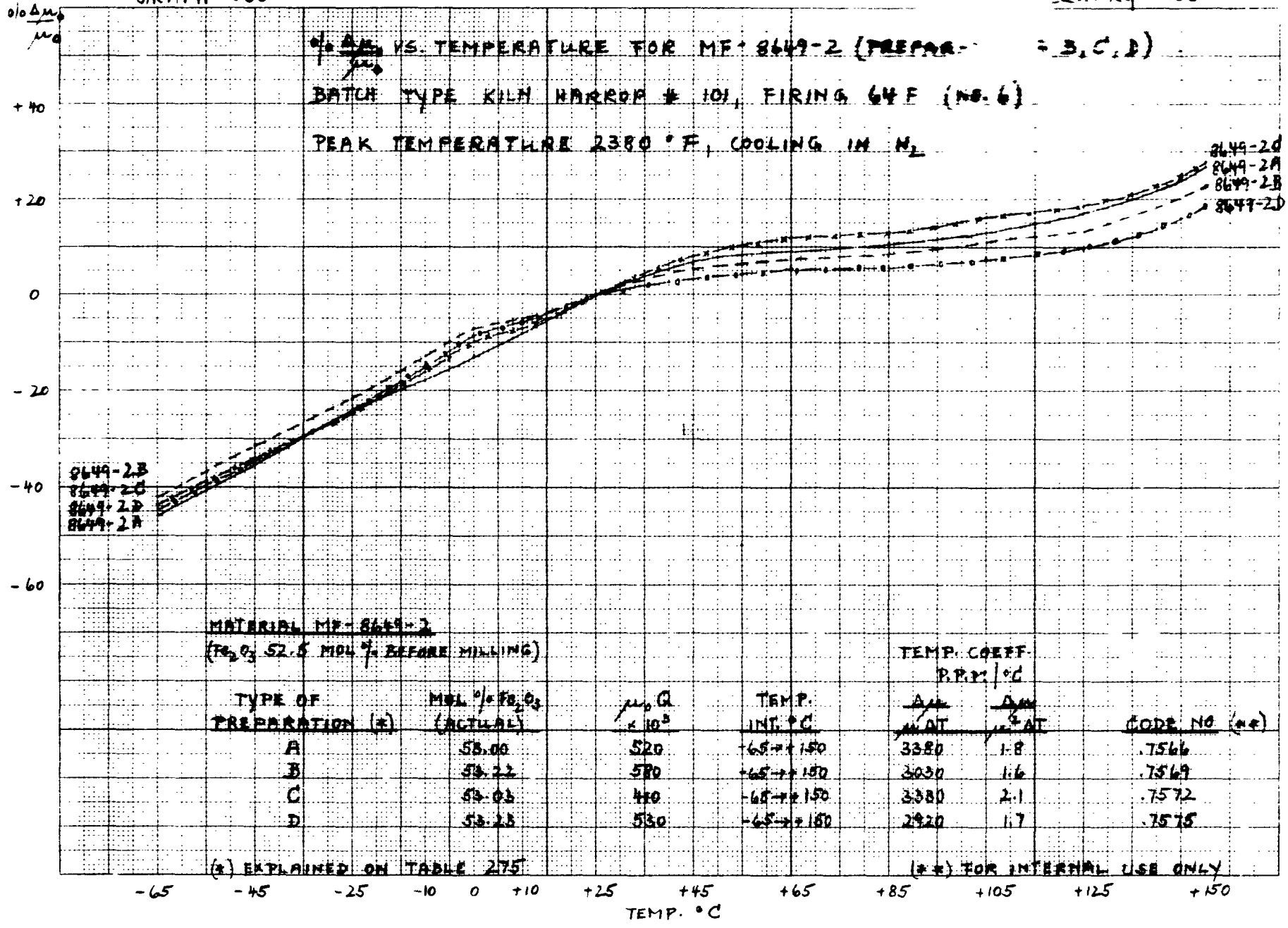

MATERIAL MF-8649-2
(Fe_2O_3 52.6 MOL % BEFORE MILLING)

TYPE OF PREPARATION (*)	MOL % Fe_2O_3 (ACTUAL)	$\mu_0 G \times 10^3$	TEMP. INT. °C	TEMP. COEFF P.P.M./°C $\frac{\Delta\mu}{\mu}$ AT	$\frac{\Delta\mu}{\mu^2}$ AT	CODE NO (**)
A	53.00	520	+65→+150	3380	1.8	.7566
B	53.22	580	+65→+150	3030	1.6	.7569
C	53.03	440	-65→+150	3380	2.1	.7572
D	53.28	530	-65→+150	2920	1.7	.7575

(*) EXPLAINED ON TABLE 275

(**) FOR INTERNAL USE ONLY

GRAPH 601

FEBRUARY 1963

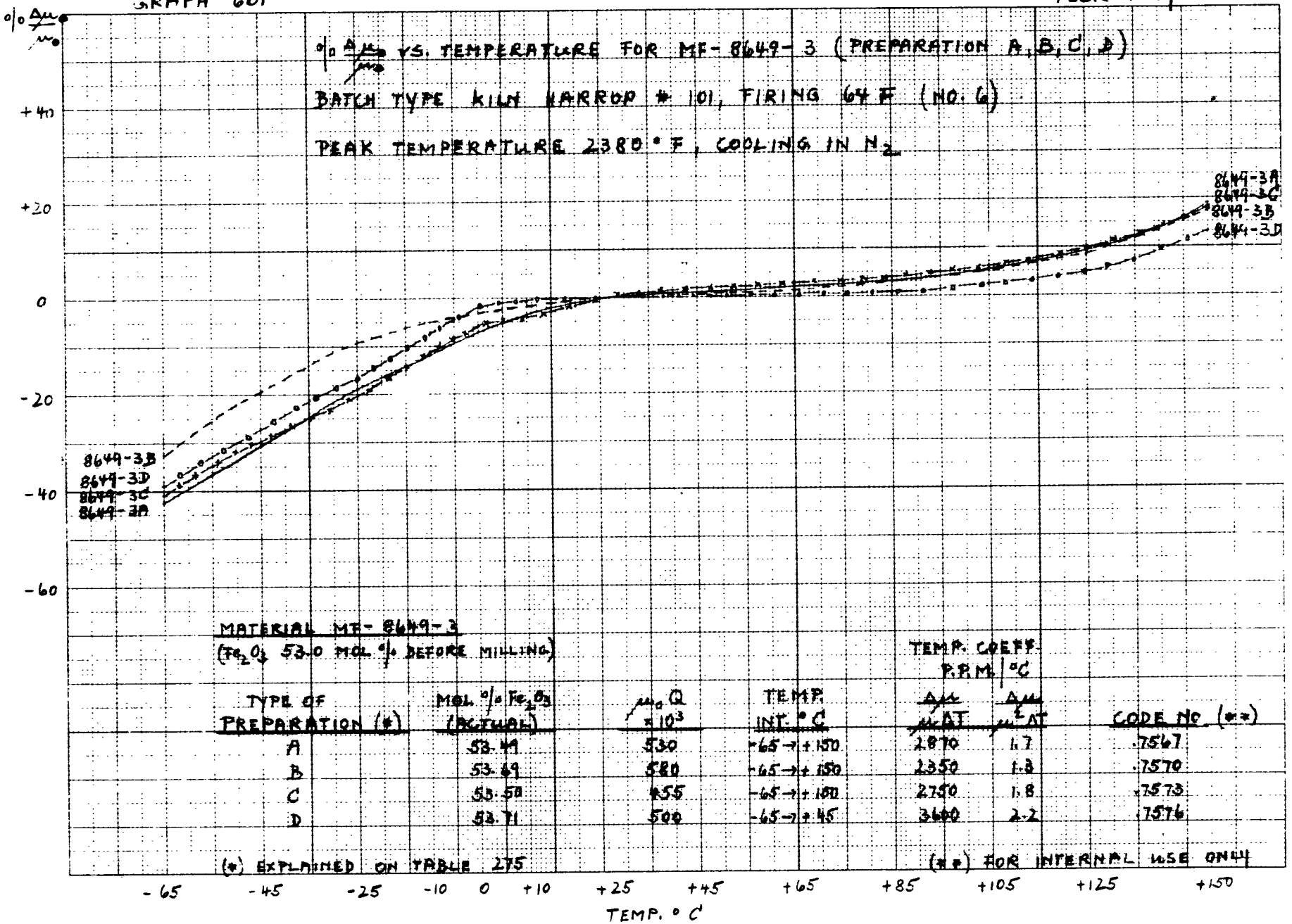

MATERIAL MF-8649-3

(Fe_2O_3 53.0 MOL % BEFORE MILLING)

TYPE OF PREPARATION (*)	MOL % Fe_2O_3 (ACTUAL)	$\mu_0 Q \times 10^3$	TEMP. INT. ° C	TEMP. COEFF. P.P.M. / °C $\frac{\Delta\mu}{\mu}$ AT	$\frac{\Delta\mu}{\mu}$ AT	CODE NO (**)
A	53.44	530	-65 → +150	2870	1.7	7567
B	53.69	580	-65 → +150	2350	1.3	7570
C	53.50	455	-65 → +100	2750	1.8	7573
D	53.71	500	-65 → +45	3600	2.2	7576

(*) EXPLAINED ON TABLE 275

(**) FOR INTERNAL USE ONLY

Graph 602

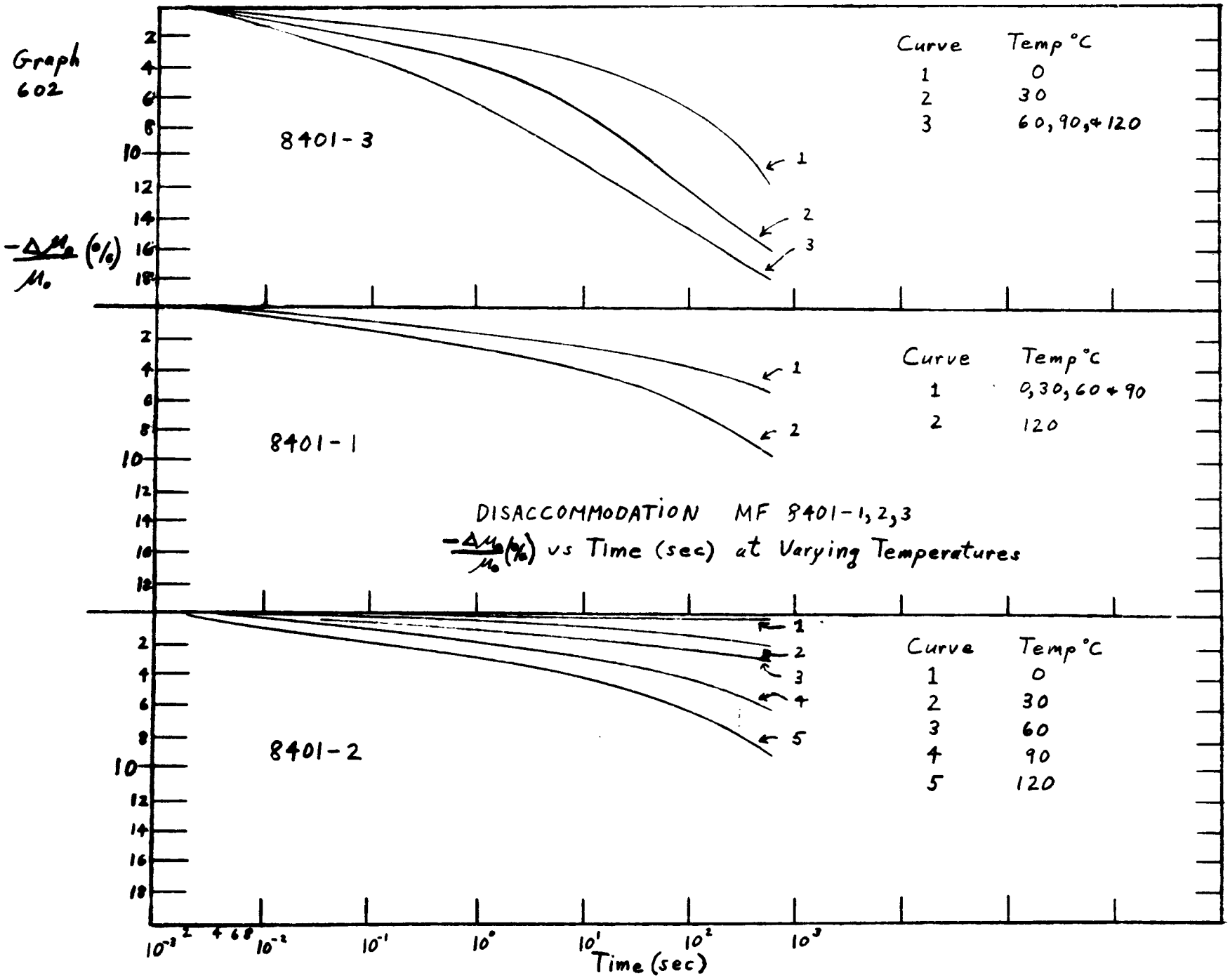

DISACCOMMODATION MF 8401-1, 2, 3

$-\frac{\Delta\mu_a}{\mu_0}$ (%) vs Time (sec) at Varying Temperatures

Graph 603

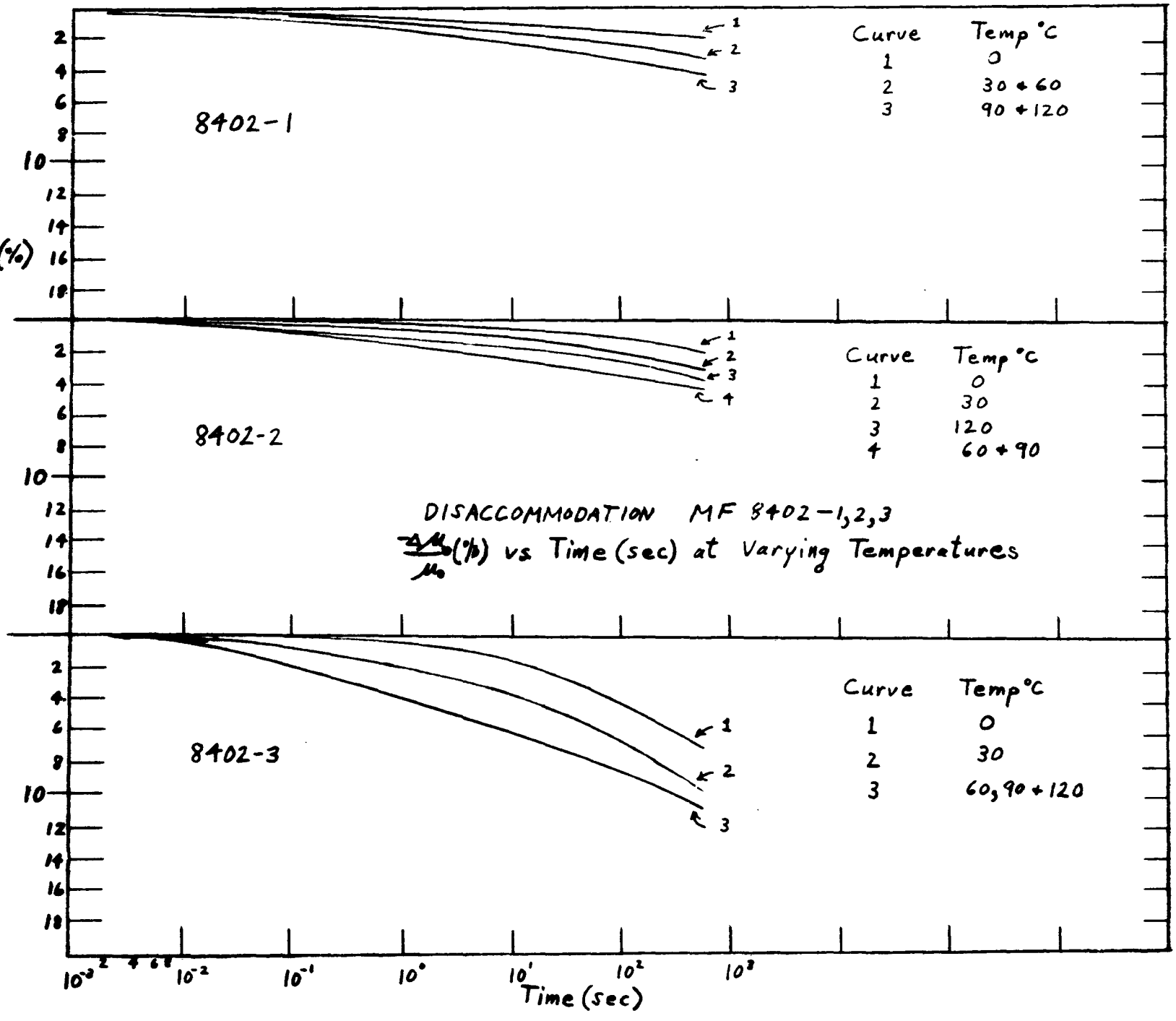

$-\frac{\Delta\mu}{\mu_0}$ (%)

DISACCOMMODATION MF 8402-1,2,3

$\frac{\Delta\mu}{\mu_0}$ (%) vs Time (sec) at Varying Temperatures

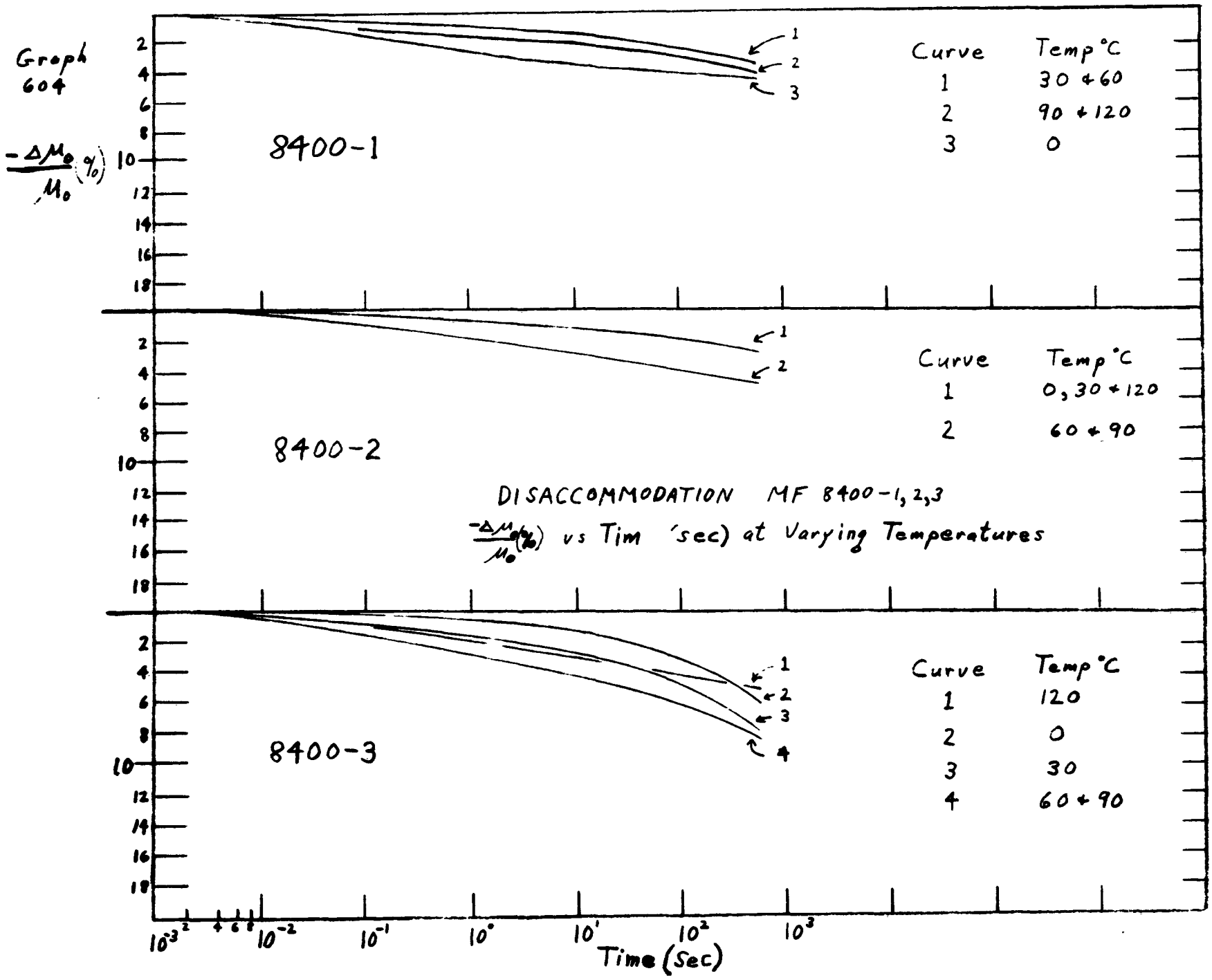
Graph 604
$\frac{-\Delta M_o}{M_o}$ (%)
8400-1
Curve Temp °C
1 30 + 60
2 90 + 120
3 0
8400-2
Curve Temp °C
1 0, 30 + 120
2 60 + 90
8400-3
Curve Temp °C
1 120
2 0
3 30
4 60 + 90
DISACCOMMODATION MF 8400-1, 2, 3
$\frac{-\Delta M_o}{M_o}$ (%) vs Tim (sec) at Varying Temperatures
Time (Sec)

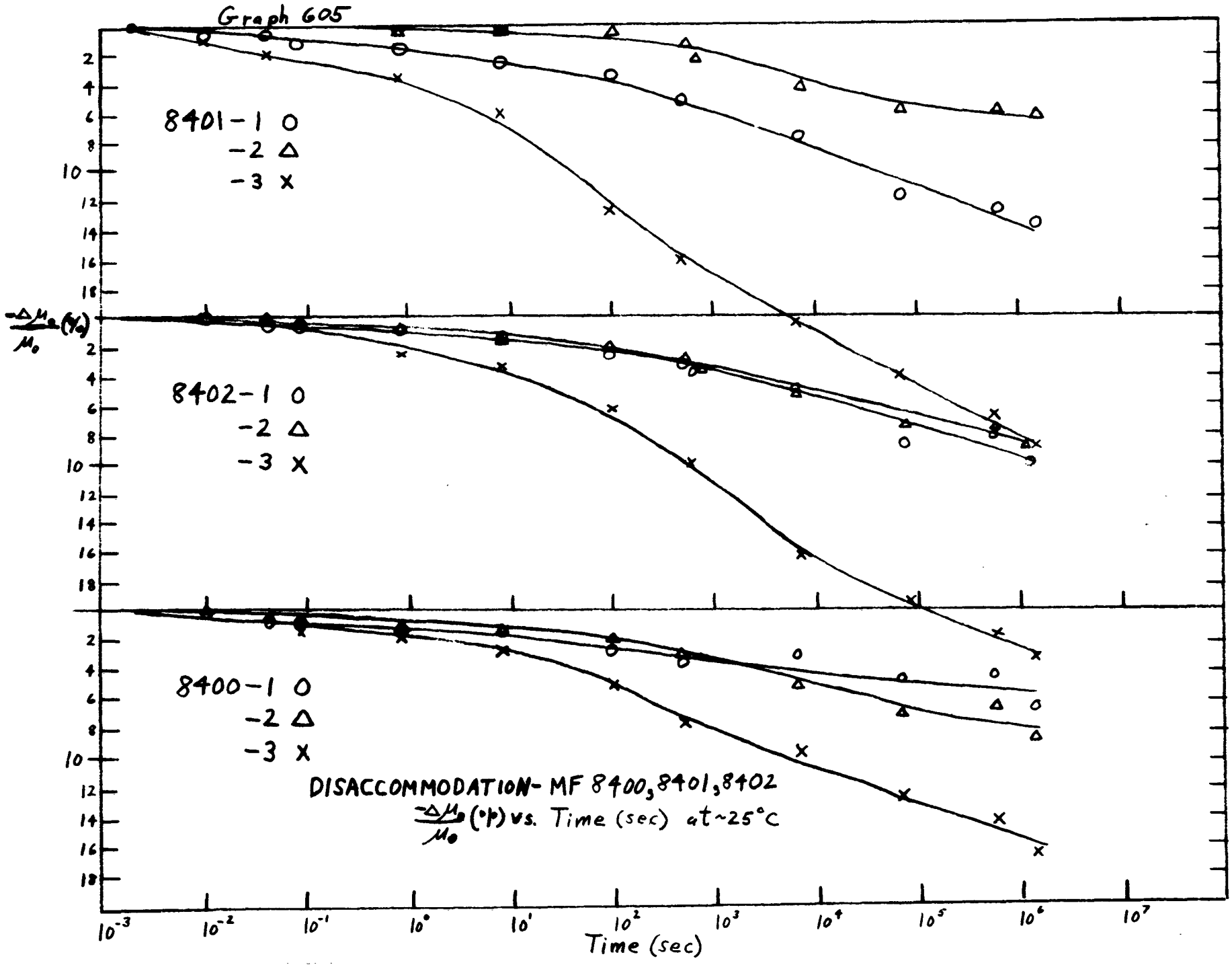
Graph 605
8401-1 O
-2 Δ
-3 X
8402-1 O
-2 Δ
-3 X
8400-1 O
-2 Δ
-3 X
$\frac{-\Delta\mu_o}{\mu_o}$ (%)
DISACCOMMODATION- MF 8400, 8401, 8402
$\frac{-\Delta\mu_o}{\mu_o}$ (%) vs. Time (sec) at ~25°C
Time (sec)

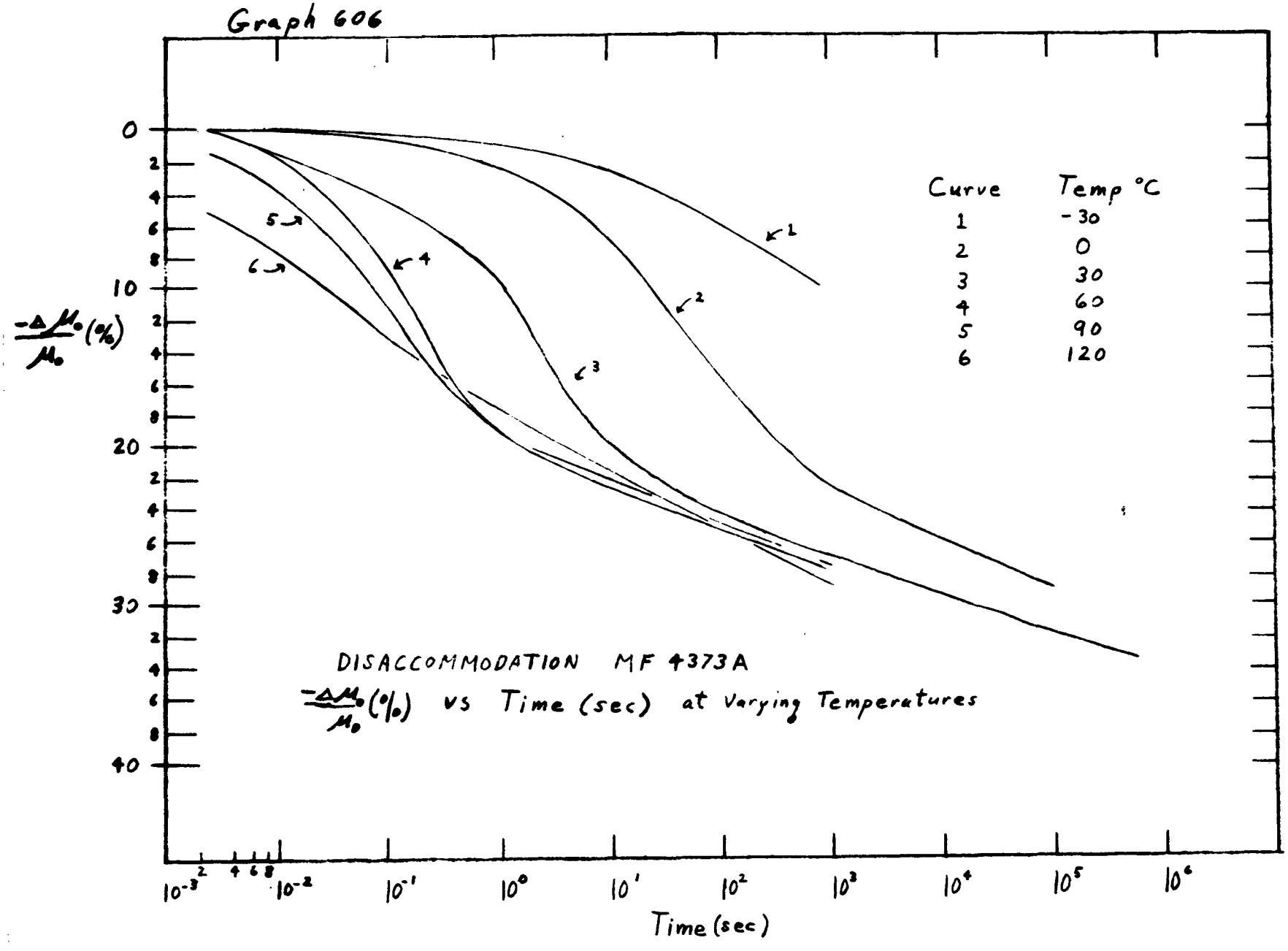
Graph 606
0
2
4
6
8
10
2
4
6
8
20
2
4
6
8
30
2
4
6
8
40
$\frac{-\Delta\mu_0}{\mu_0}$(%)
Curve
Temp °C
1
-30
2
0
3
30
4
60
5
90
6
120
1
2
3
4
5
6
DISACCOMMODATION MF 4373A
$\frac{-\Delta\mu_0}{\mu_0}$(%) vs Time (sec) at Varying Temperatures
10^{-3}
2
4
6
8
10^{-2}
10^{-1}
10^{0}
10^{1}
10^{2}
10^{3}
10^{4}
10^{5}
10^{6}
Time (sec)

Graph 607

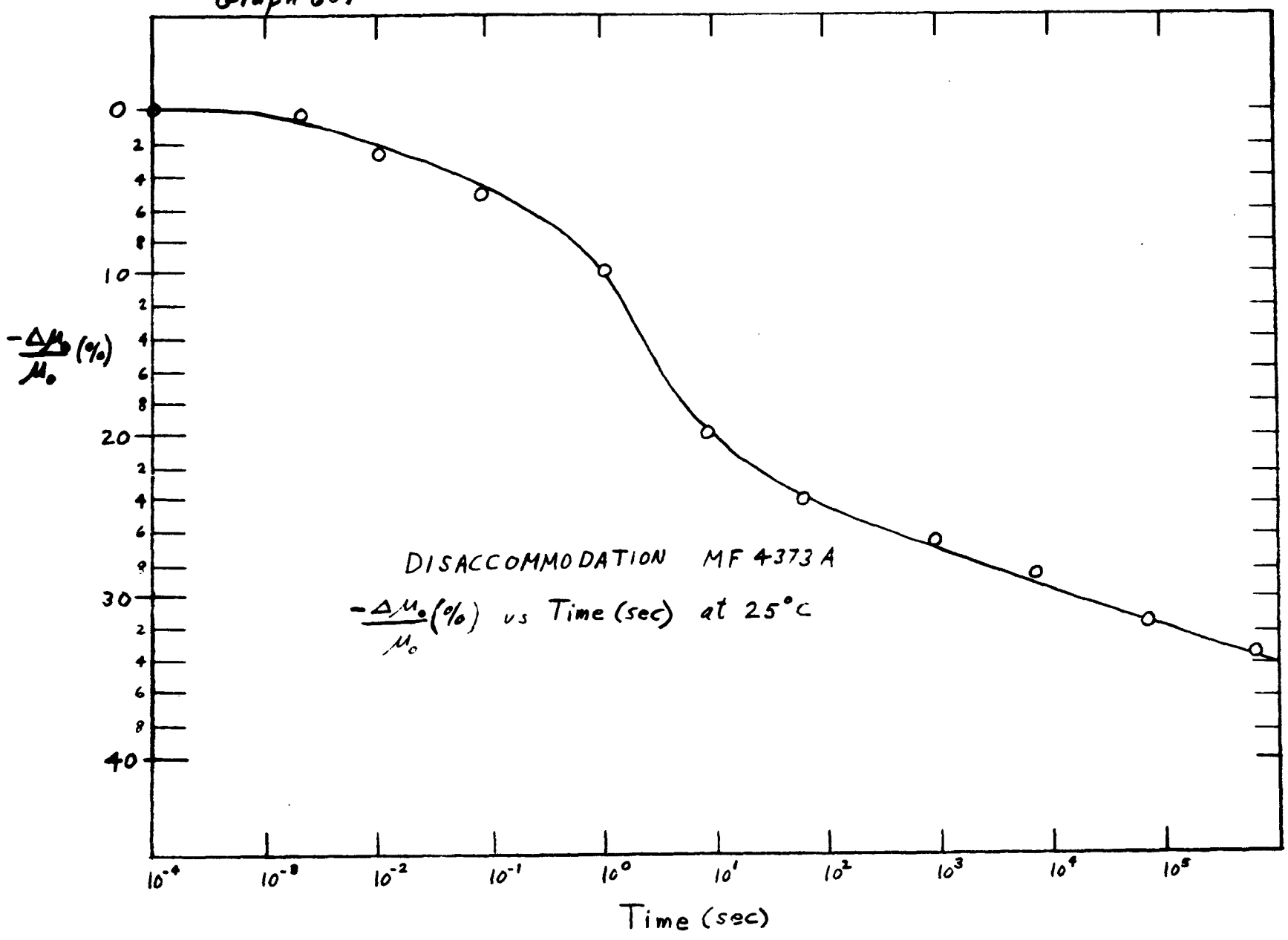
0
2
4
6
8
10
2
4
6
8
20
2
4
6
8
30
2
4
6
8
40
$-\frac{\Delta\mu_0}{\mu_0}$ (%)
DISACCOMMODATION MF 4373 A
$-\frac{\Delta\mu_0}{\mu_0}$ (%) vs Time (sec) at 25°C
10^{-4}
10^{-3}
10^{-2}
10^{-1}
10^{0}
10^{1}
10^{2}
10^{3}
10^{4}
10^{5}
Time (sec)

GRAPH 608

FEBRUARY, 1963

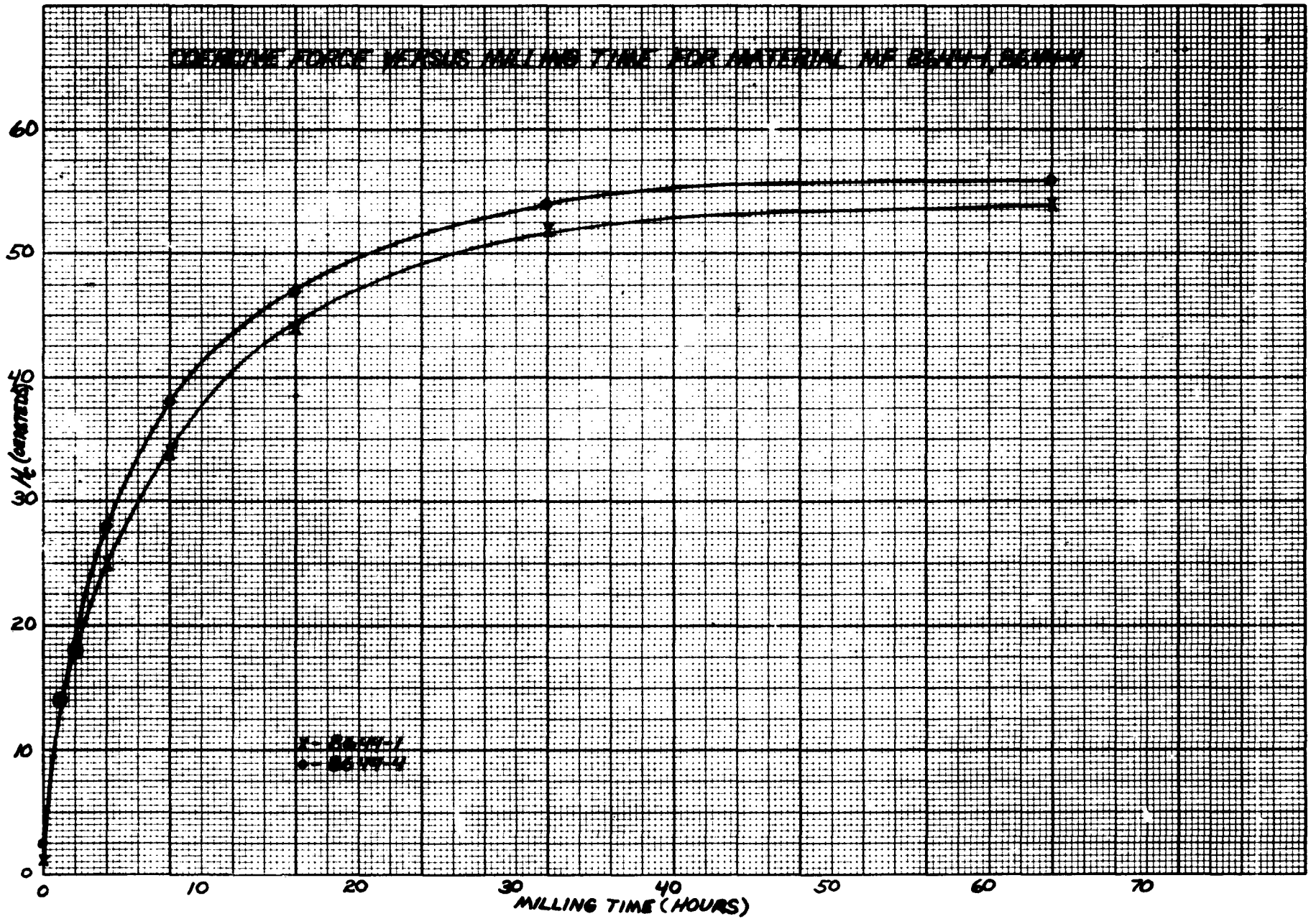

GRAPH 609

FEBRUARY, 1963

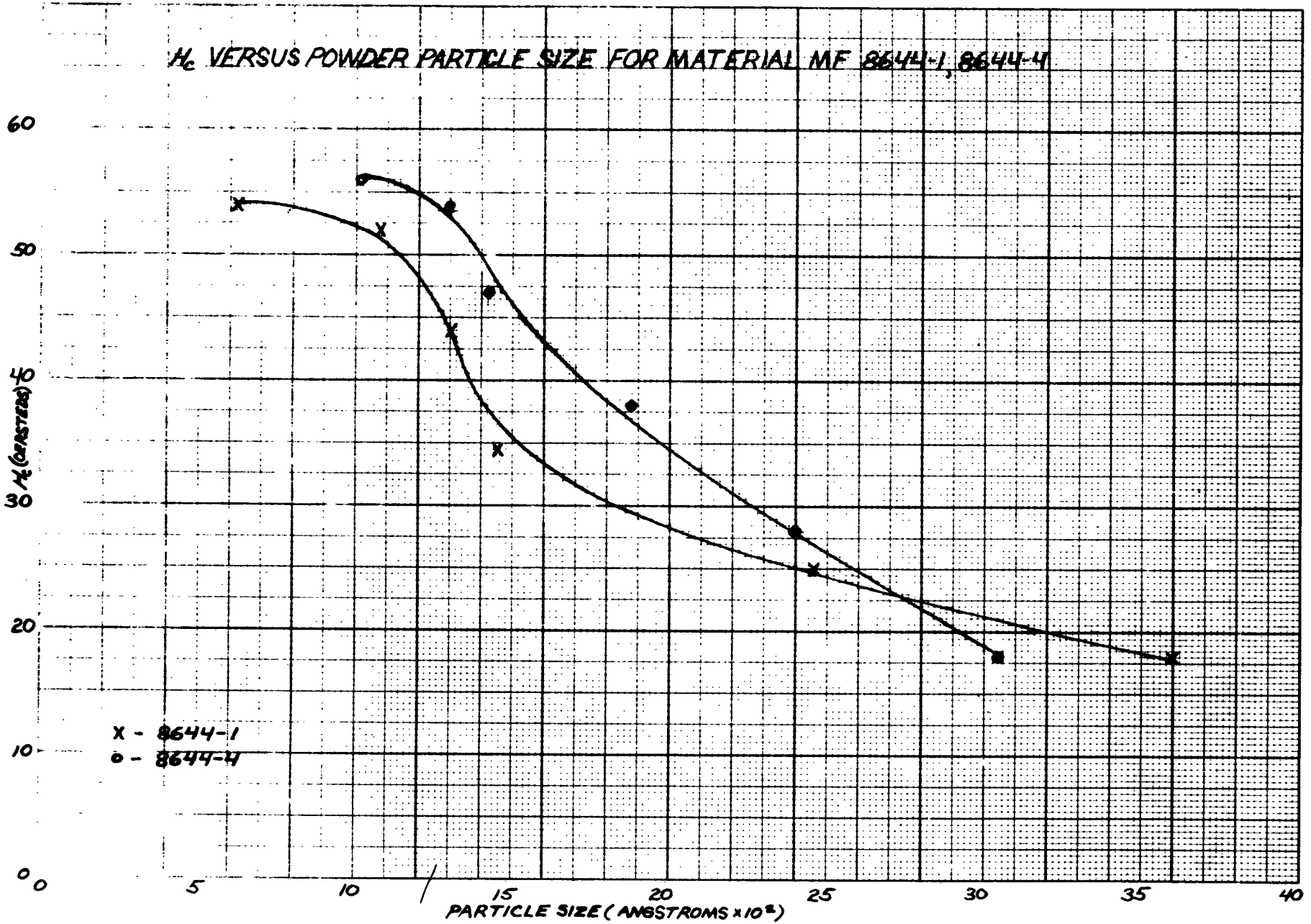

GRAPH 6/0

FEBRUARY 1963

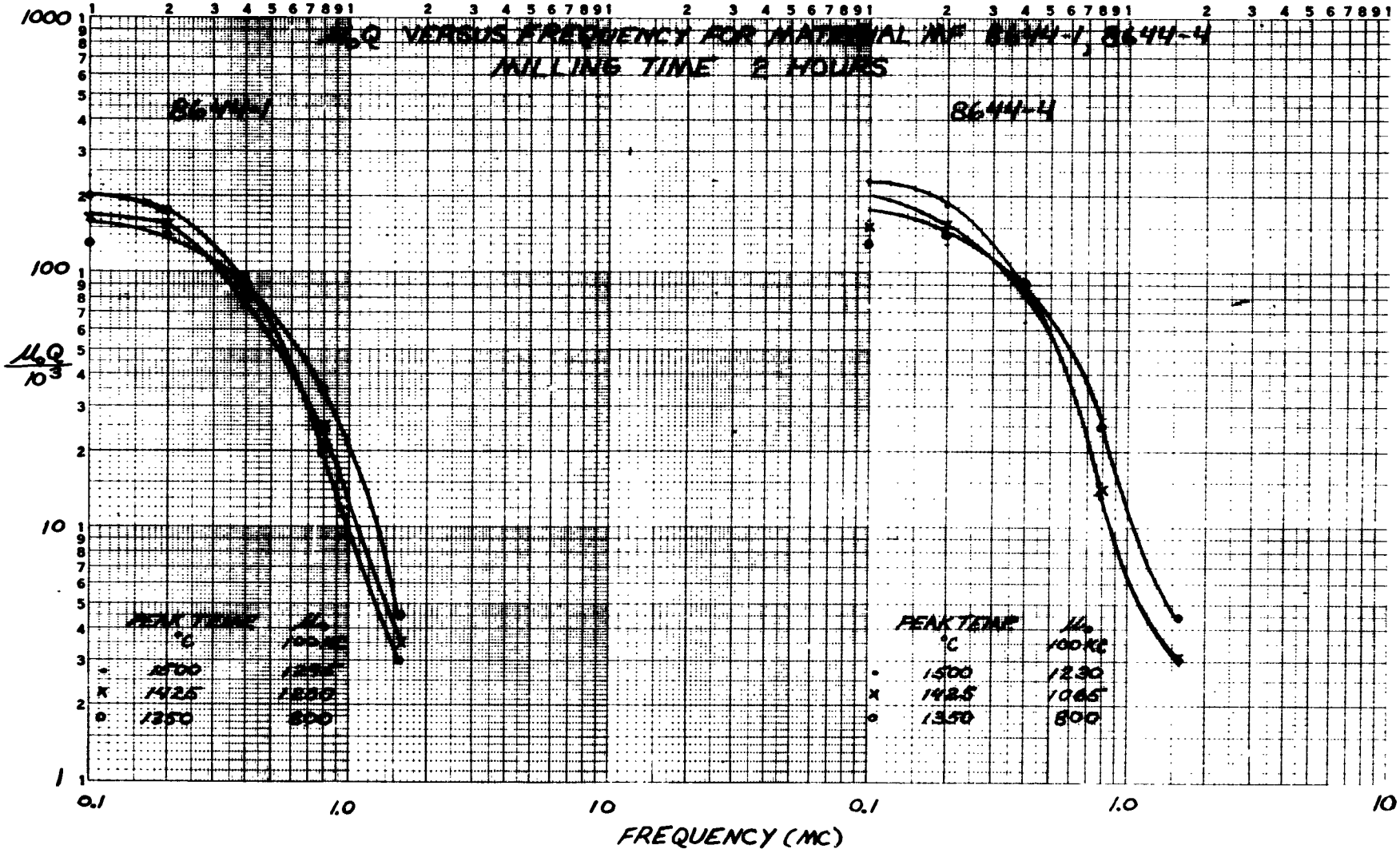

GRAPH 611

FEBRUARY 1963

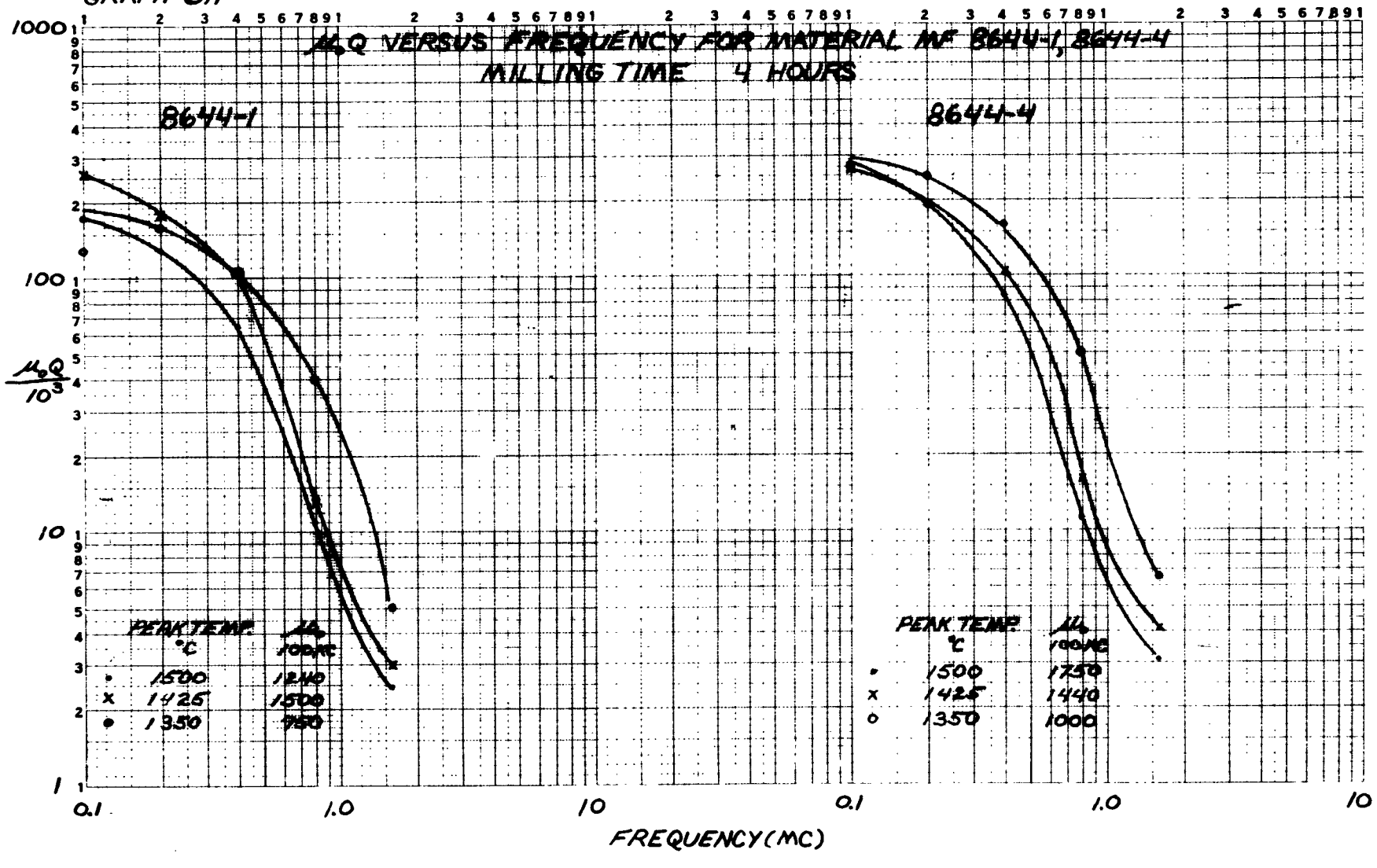

GRAPH 612

FEBRUARY 1963

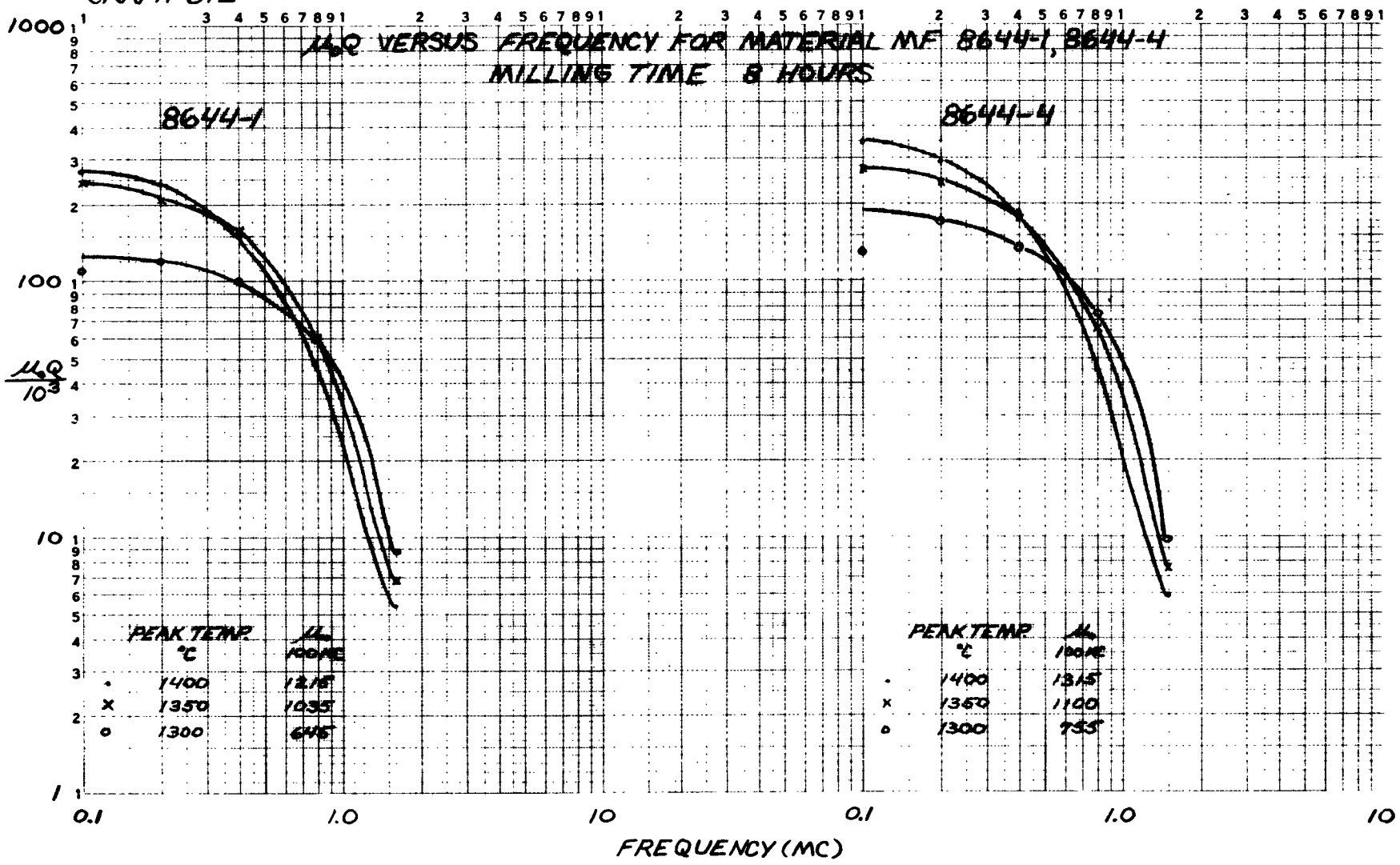

GRAPH 613

FEBRUARY 1963

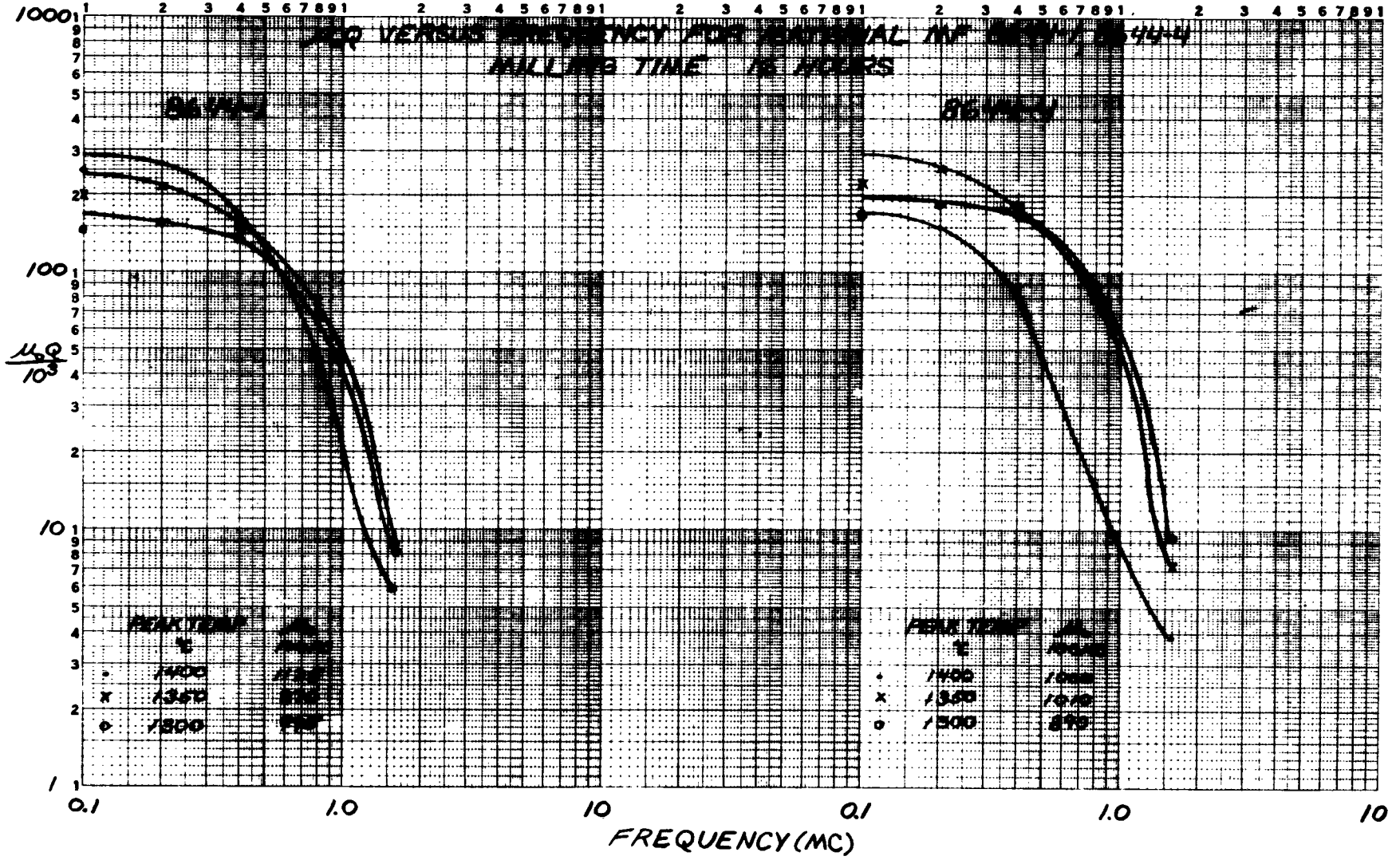

GRAPH 614

FEBRUARY 1963

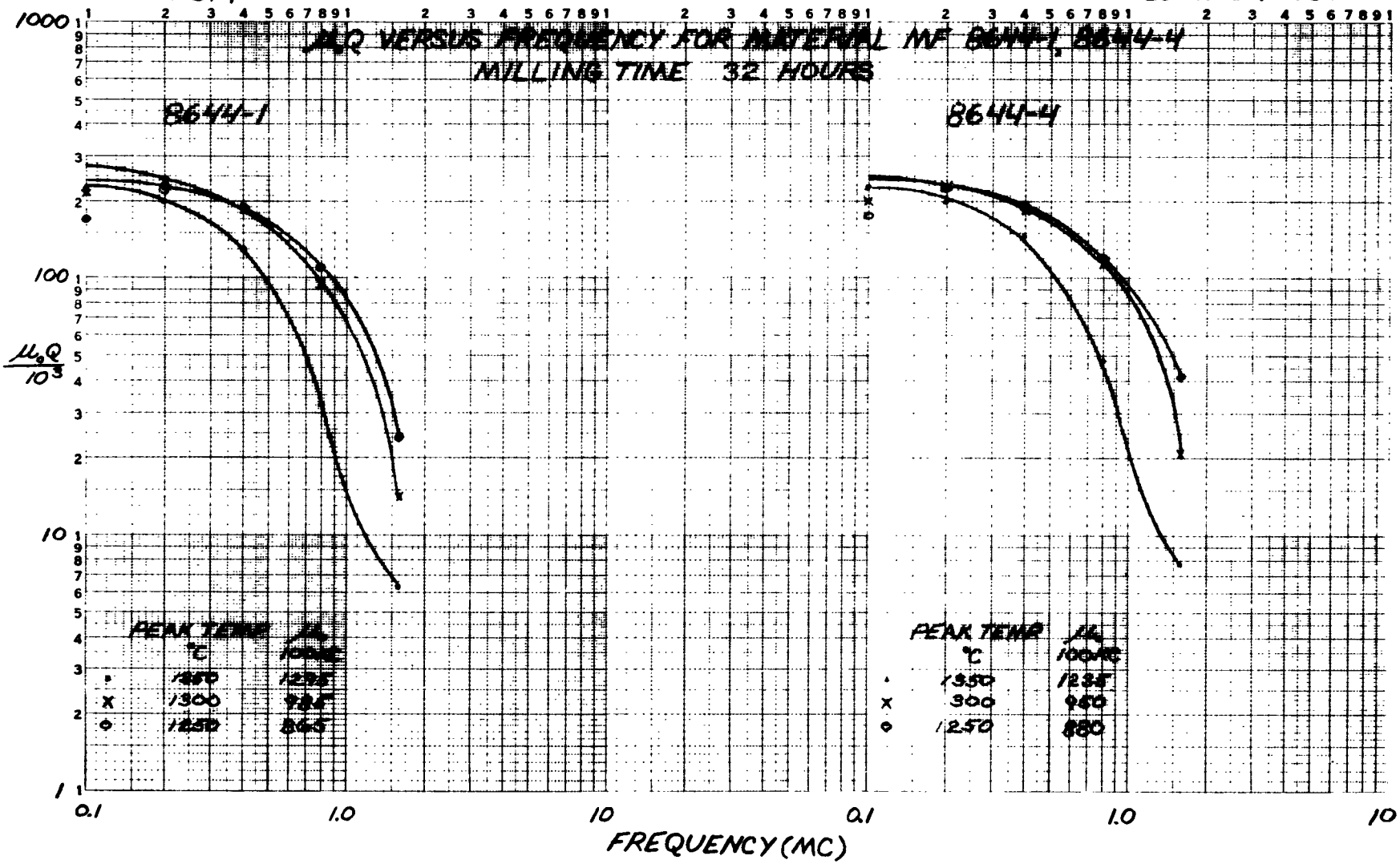

GRAPH 615

FEBRUARY 1963

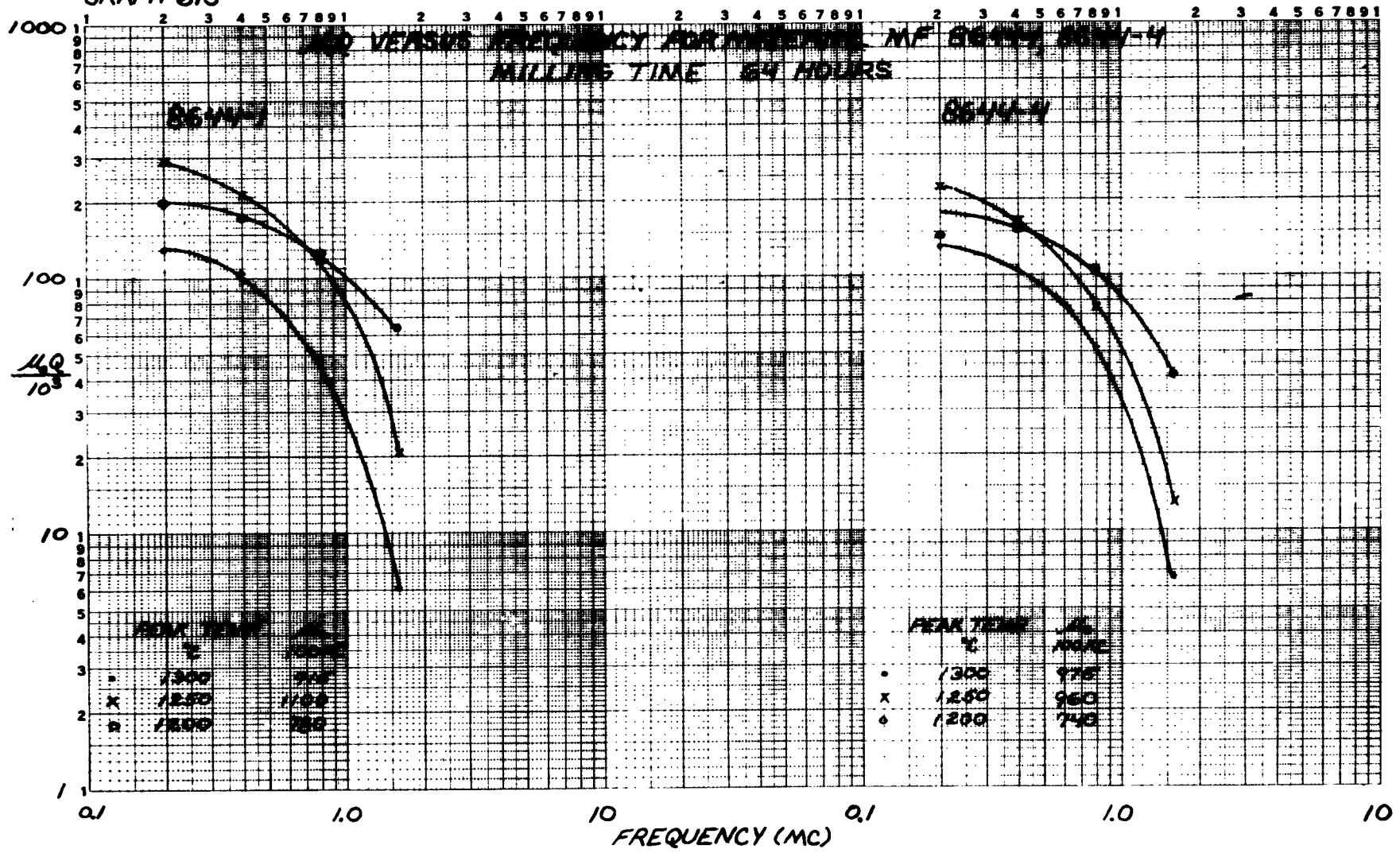

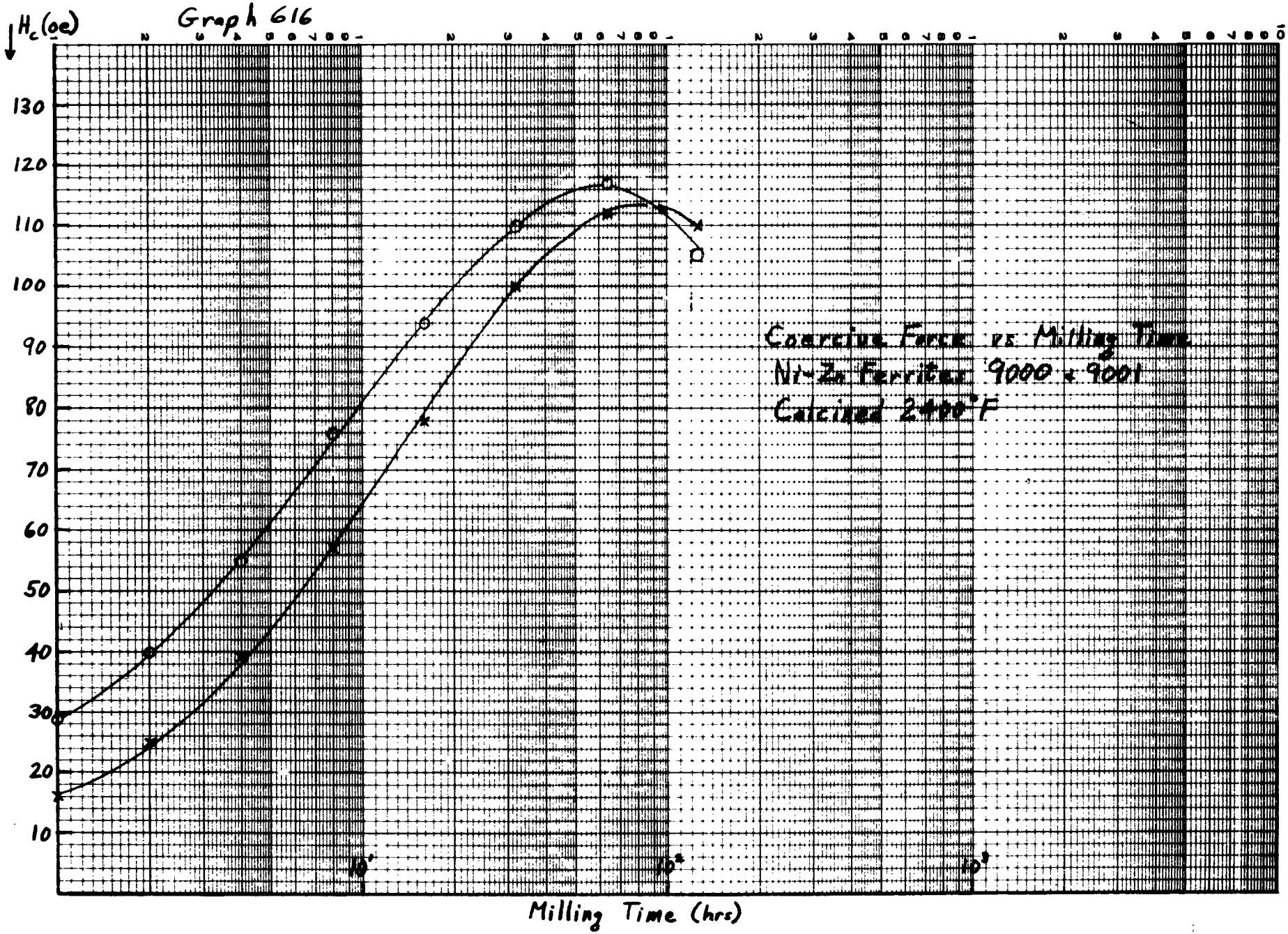
Graph 616
H_c (oe)
130
120
110
100
90
80
70
60
50
40
30
20
10
Coercive Force vs Milling Time
Ni-Zn Ferrites 9000 & 9001
Calcined 2400°F
Milling Time (hrs)

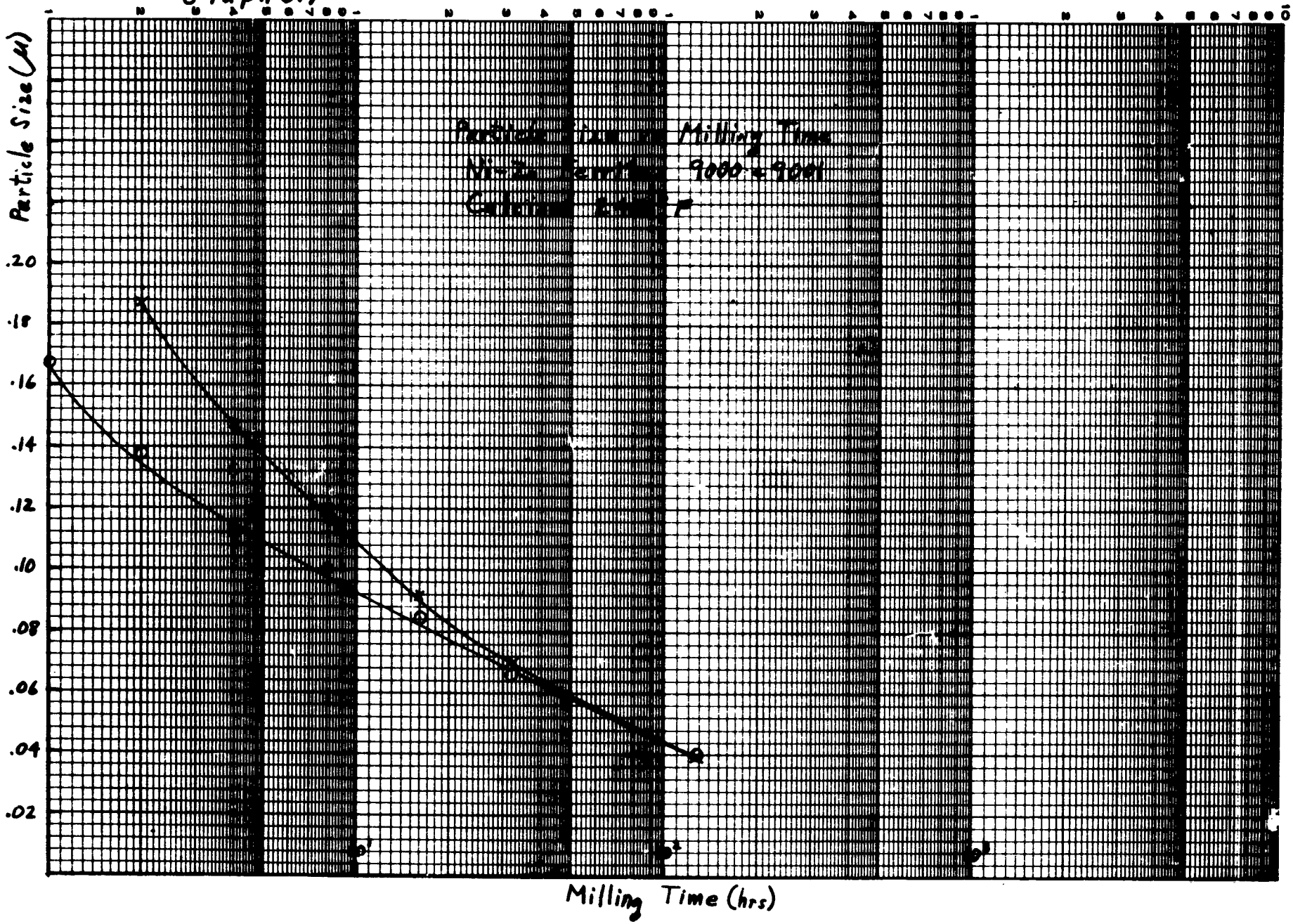
Graph 617
Particle Size (μ)
.20
.18
.16
.14
.12
.10
.08
.06
.04
.02
Milling Time
9000 : 900
Milling Time (hrs)

Graph 618

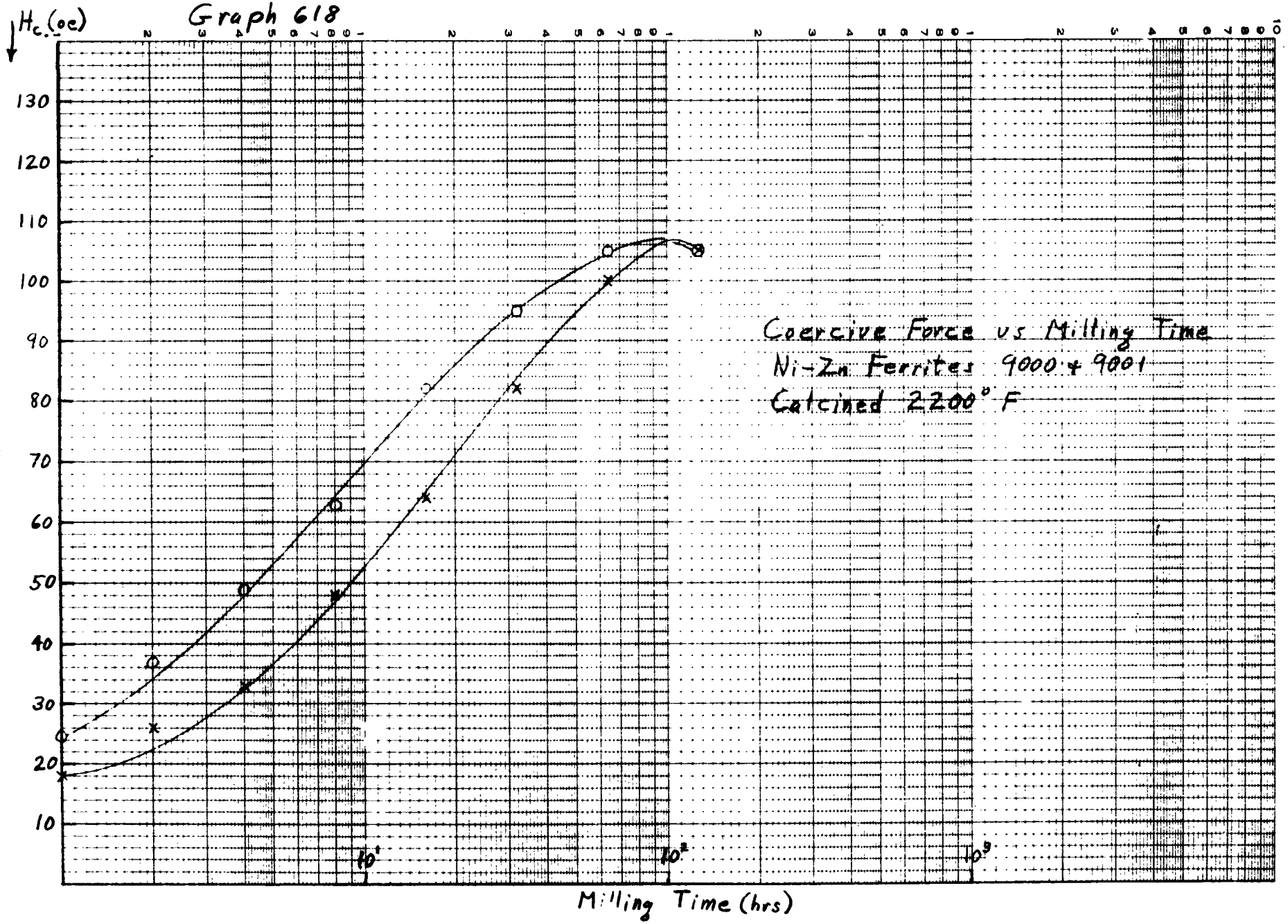
H_c (oe)
130
120
110
100
90
80
70
60
50
40
30
20
10
10^1
10^2
10^3
Milling Time (hrs)
Coercive Force vs Milling Time
Ni-Zn Ferrites 9000 + 9001
Calcined 2200° F

TABLE 275

TEST SERIES - MF-8649

a) SCHEDULE OF DIFFERENT TYPES OF PREPARATION AND ITS EFFECT UPON THE IRON OXIDE RATIO

MF-8649	BEFORE AND Fe_2O_3 MOL %	Fe_2O_3 MOL % AFTER MILLING TYPE OF PREPARATION "A"	"B"	"C"	"D"
-1	52.0	52.55	52.74	52.56	52.76
-2	52.5	53.00	53.22	53.03	53.23
-3	53.0	53.49	53.69	53.50	53.71
CALCINING TEMP: = °F		2000	2000	2300	2300
GRINDING TIME : = HRS		18	36	18	36

TYPE OF STEEL MILL: "BACILLI"

CHARGE: 500 g OF MATERIAL - 4 kg OF STEEL BALLS 1/2" DIAMETER

b) SCHEDULE OF FIRINGS

FIRING NO.	KILN	PEAK TEMP.	COOLING
1	103	2480°F	NITROGEN
2	58F	2400°F	"
3	60F	2450°F	"
5	63F	2350°F	"
6	64F	2380°F	"

TABLE 276

MAGNETIC PROPERTIES OF MF-8649-1 OBTAINED FROM FOUR DIFFERENT TYPES OF PREPARATION (*) AND FROM FIVE DIFFERENT FIRINGS (*)

MEASUREMENTS OF μ_o AND Q AT FREQUENCIES OF FROM 100 TO 300 KC/S

(*) PREPAR.	(*) FIRING	100 KC/S μ_o	100 KC/S Q	100 KC/S μ_oQ x10^3	200 KC/S μ_o	200 KC/S Q	200 KC/S μ_oQ x10^3	300 KC/S μ_o	300 KC/S Q	300 KC/S μ_oQ x10^3	CODE NO. (**) III
"A"	1	2060	160	330	2130	55	115	2220	20	45	.7485
	2	1840	200	370	1880	120	225	1940	75	145	.7512
	3	1580	235	370	1600	145	230	1640	100	165	.7525
	5	1910	195	370	1930	120	230	2000	75	150	.7549
	6	1670	235	375	1700	150	255	1730	100	170	.7565
	Average:	1810	205	365	1850	120	210	1905	75	135	
"B"	1	2020	165	335	260	85	175	2140	35	75	.7488
	2	1350	255	345	1380	165	225	1390	120	165	.7515
	3	1100	270	295	1120	175	195	1130	130	145	.7528
	5	1110	195	215	1130	115	130	1150	80	90	.7552
	6	1680	275	460	1700	175	300	1730	120	205	.7568
	Average:	1450	230	330	1480	145	205	1510	95	135	
"C"	1	1690	180	305	1720	90	155	1780	35	60	.7491
	2	1770	205	365	1800	125	225	1850	75	140	.7518
	3	1660	215	355	1690	135	230	1730	90	155	.7531
	5	1800	205	370	1840	115	210	1880	85	160	.7555
	6	1570	235	370	1620	155	250	1640	105	170	.7571
	Average:	1700	210	350	1735	125	215	1775	80	135	
"D"	1	1430	185	265	1460	120	175	1490	70	105	.7494
	2	1900	240	455	1950	135	265	2000	80	160	.7521
	3	1540	250	385	1570	165	260	1595	115	180	.7534
	5	1570	235	370	1610	150	240	1640	100	165	.7558
	6	1625	260	420	1650	190	315	1680	130	220	.7574
	Average:	1610	235	380	1650	150	250	1680	100	165	

* See Table 275

** For the purpose of identification of sample only.

TABLE 277

MAGNETIC PROPERTIES OF MF-8649-2 OBTAINED FROM FOUR DIFFERENT TYPES OF PREPARATION (*) AND FROM FIVE DIFFERENT FIRINGS (*)

MEASUREMENTS OF μ_o AND Q AT FREQUENCIES OF FROM 100 TO 300 KC/S

(*) PREPAR.	(*) FIRING	100 KC/S μ_o	100 KC/S Q	100 KC/S μ_oQ x10^3	200 KC/S μ_o	200 KC/S Q	200 KC/S μ_oQ x10^3	300 KC/S μ_o	300 KC/S Q	300 KC/S μ_oQ x10^3	CODE NO. (**) III
"A"	1	1980	140	275	2030	75	150	2140	30	65	.7486
	2	1950	255	495	1990	145	290	2060	70	145	.7513
	3	1800	260	470	1840	160	295	1895	105	200	.7526
	5	1850	235	435	1880	145	270	1960	75	145	.7550
	6	1890	275	520	1920	160	305	1980	90	180	.7566
	Average:	1895	235	440	1930	140	260	2070	75	145	
"B"	1	1830	140	255	1850	85	155	1900	55	105	.7489
	2	1750	235	410	1770	140	250	1820	90	165	.7516
	3	1220	315	385	1245	210	260	1255	145	180	.7529
	5	1170	205	240	1200	120	145	1215	80	95	.7553
	6	1840	315	580	1860	195	360	1900	130	245	.7569
	Average:	1560	240	375	1585	150	235	1620	100	160	
"C"	1	1450	165	240	1470	100	145	1505	65	100	.7492
	2	1760	260	455	1790	155	275	1840	85	155	.7519
	3	1700	260	440	1725	165	285	1760	115	200	.7532
	5	1750	250	440	1780	155	275	1830	85	155	.7556
	6	1530	270	410	1570	195	305	1590	130	205	.7572
	Average:	1640	240	385	1665	155	245	1705	95	165	
"D"	1	1260	160	200	1280	110	140	1295	80	105	.7495
	2	1735	260	450	1770	175	310	1800	115	205	.7522
	3	1830	280	510	1875	180	335	1910	120	230	.7535
	5	1980	185	365	2010	105	210	2070	65	135	.7559
	6	1730	305	530	1780	220	390	1800	140	250	.7575
	Average:	1710	240	410	1740	160	275	1775	105	185	

* See Table 275

** For the purpose of identification of sample only.

TABLE 278

MAGNETIC PROPERTIES OF MF-8649-3 OBTAINED FROM FOUR DIFFERENT TYPES OF PREPARATION (*) AND FROM FIVE DIFFERENT FIRINGS (*)

MEASUREMENTS OF μ_c AND Q AT FREQUENCIES OF FROM 100 TO 300 KC/S

(*) PREPAR.	(*) FIRING	100 KC/S μ_o	100 KC/S Q	100 KC/S μ_oQ x10^3	200 KC/S μ_o	200 KC/S Q	200 KC/S μ_oQ x10^3	300 KC/S μ_o	300 KC/S Q	300 KC/S μ_oQ x10^3	CODE NO. (**) III
"A"	1	1620	120	195	1670	70	115	1710	45	75	.7487
	2	1780	270	480	1820	165	300	1845	110	200	.7514
	3	1780	320	570	1820	200	365	1860	135	250	.7527
	5	1760	225	395	1780	140	250	1840	90	165	.7551
	6	1730	305	530	1750	195	340	1780	130	230	.7567
	Average:	1735	250	375	1770	155	275	1810	100	185	
"B"	1	1660	125	205	1695	80	135	1735	55	95	.7490
	2	1580	300	475	1600	185	295	1630	130	210	.7517
	3	1270	360	455	1300	235	305	1305	170	220	.7530
	5	1130	240	270	1146	155	175	1160	110	125	.7554
	6	1740	335	580	1790	210	375	1820	150	270	.7570
	Average:	1475	270	395	1505	175	260	1530	125	185	
"C"	1	1360	140	190	1500	100	150	1400	65	90	.7493
	2	1595	250	400	1620	165	265	1650	110	180	.7520
	3	1740	295	510	1760	195	345	1795	130	235	.7533
	5	1590	235	375	1610	175	280	1650	105	175	.7557
	6	1545	295	455	1570	210	330	1600	150	240	.7573
	Average:	1585	245	385	1610	170	275	1620	110	185	
"D"	1	1230	140	170	1245	100	125	1265	70	90	.7496
	2	1590	260	415	1625	165	270	1650	120	200	.7523
	3	1750	300	520	1795	200	360	1815	140	255	.7536
	5	1680	195	325	1720	130	225	1750	90	155	.7560
	6	1610	310	500	1650	230	380	1670	160	265	.7576
	Average:	1570	240	385	1605	165	270	1630	115	195	

* See Table 275

** For the purpose of identification of sample only.

UNITED STATES ARMY ELECTRONICS RESEARCH & DEVELOPMENT AGENCY
STANDARD DISTRIBUTION LIST
RESEARCH AND DEVELOPMENT CONTRACT REPORTS

COPIES	
1	OASD (R&E) ATTN: Technical Library, Room 3E1065, The Pentagon, Washington 25, D. C.
1	Chief of Research and Development, OCS, Department of the Army, Washington 25, D. C.
1	Commanding General, U. S. Army Materiel Command, ATTN: R&E Directorate Washington 25, D. C.
1	Commanding General, U. S. Army Electronics Command, ATTN: AMSEL-AD Fort Monmouth, N. J.
1	Director, U. S. Naval Research Laboratory, ATTN: Code 2027, Washington 25, D. C.
1	Commander, Aeronautical Systems Division, ATTN: ASAPRL, Wright-Patterson Air Force Base, Ohio
1	Hq., Electronic Systems Division, ATTN: ESAL, L. G. Hanscom Field Bedford, Massachusetts
1	Commander, Air Force Cambridge Research Laboratories, ATTN: CRO L. G. Hanscom Field, Bedford, Massachusetts
1	Commander, Air Force Command & Control Development Division, ATTN: CRZC L. G. Hanscom Field, Bedford, Massachusetts
1	Commander, Rome Air Development Center, ATTN: RAALD Griffiss Air Force Base, New York
10	Commander, Armed Services Technical Information Agency, ATTN: TISIA Arlington Hall Station, Arlington 12, Virginia
2	Chief, U. S. Army Security Agency, Arlington Hall Station, Arlington 12, Virginia
1	Deputy President, U. S. Army Security Agency Board, Arlington Hall Station, Arlington 12, Virginia
1	Commanding Officer, Harry Diamond Laboratories, ATTN: Library, Room 211, Building 92, Washington 25, D. C.

(Continued)

COPIES

1 Corps of Engineers Liaison Office, U. S. Army Electronics Research & Development Laboratory, Fort Monmouth, N. J.

1 AFSC Scientific/Technical Liaison Office, U. S. Naval Air Development Center, Johnsville, Pennsylvania

1 USAELRDL Liaison Office, Rome Air Development Center, ATTN: RAOL Griffiss Air Force Base, New York

1 Commanding Officer, U. S. Army Electronics Materiel Support Agency, ATTN: SELMS-ADJ, Fort Monmouth, N. J.

1 Marine Corps Liaison Office, U. S. Army Electronics Research & Development Laboratory, ATTN: SELRA/LNR, Fort Monmouth, N. J.

1 Commanding Officer, U.S. Army Electronics Research & Development Laboratory, ATTN: Director of Research or Engineering, Fort Monmouth, New Jersey

1 Commanding Officer, U. S. Army Electronics Research & Development Laboratory, Attn: Technical Documents Center, Fort Monmouth, New Jersey

1 Commanding Officer, U.S. Army Electronics Research & Development Laboratory, ATTN: SELRA/TNR, Fort Monmouth, New Jersey

2 Advisory Group on Electron Devices, 346 Broadway, New York 13, New York

3 Commanding Officer, U. S. Army Electronics Research & Development Laboratory, ATTN: SELRA/TNR Fort Monmouth, New Jersey

(FOR RETRANSMITTAL TO ACCREDITED BRITISH AND CANADIAN GOVERNMENT REPRESENTATIVES)

1 Commanding General, U. S. Army Combat Developments Command, ATTN: CDCMR-E, Fort Belvoir, Virginia

1 Commanding Officer, U. S. Army Communications-Electronics Combat Development Agency, Fort Huachuca, Arizona

1 Director, Fort Monmouth Office, U. S. Army Communications-Electronics Combat Development Agency, Building 410, Fort Monmouth, New Jersey

1 AFSC Scientific/Technical Liaison Office, U. S. Army Electronics Research & Development Laboratory, Fort Monmouth, New Jersey

1 Commanding Officer and Director, U. S. Navy Electronics Laboratory, San Diego 52, California

(Continued)

COPIES	
1	Deputy President, U. S. Army Security Agency Board, Arlington Hall Station, Arlington 12, Virginia
1	Ordnance Corps, Frankford Arsenal, Philadelphia 37, Pennsylvania, ATTN: Library Reports Section
1	Commander, Naval Ordnance Laboratory, White Oak, Silver Springs, 19, Maryland, ATTN: Library Room -1-333
1	Chief, BuAeronautics, Dept. of the Navy, Washington 25, D. C.
1	Commanding Officer, Watertown Arsenal, Watertown, Massachusetts, Attn: OMRO
1	Commanding Officer, 9560 TSU, SIG. C, Electronics Research Unit, P.O. Box #205, Mountain View, California
1	Commanding Officer, U.S.N. Underwater Sound Laboratory, New London, Connecticut
1	M.I.T., Lincoln Laboratory, Division #6, Group #63, Lexington, Massachusetts, ATTN: Librarian
1	Task Order No. EDG6, Engineering Research Institute, University of Michigan, Ann Arbor, Michigan, ATTN: Mr. D. M. Grimes
1	General Electric Corporation, Electronics Park, Syracuse, New York ATTN: Dr. H. Rothenberg
1	M.I.T., Laboratory for Insulation Research, Cambridge 39, Massachusetts ATTN: Librarian
1	Chu Associates, P.O. Box #387, Whitcomb Avenue, Littleton, Massachusetts
1	R.C.A., Semi-Conductor & Materials Division, Somerville, New Jersey ATTN: Mr. G. Houser
1	R.C.A. Laboratories, Princeton, New Jersey, ATTN: Mr. R. L. Harvey
1	Hughes Aircraft Company, Culver City, California, ATTN: E. M. Wallace Head, Documents Group
*	Headquarters, U. S. Army Elcts. Research & Development Agency, Fort Monmouth, New Jersey, ATTN: SELRA/PEM

* Remaining Copies